iScience

CellPress
OPEN ACCESS

Article

N6-methyl-2′-deoxyadenosine promotes self-renewal of BFU-E progenitor in erythropoiesis

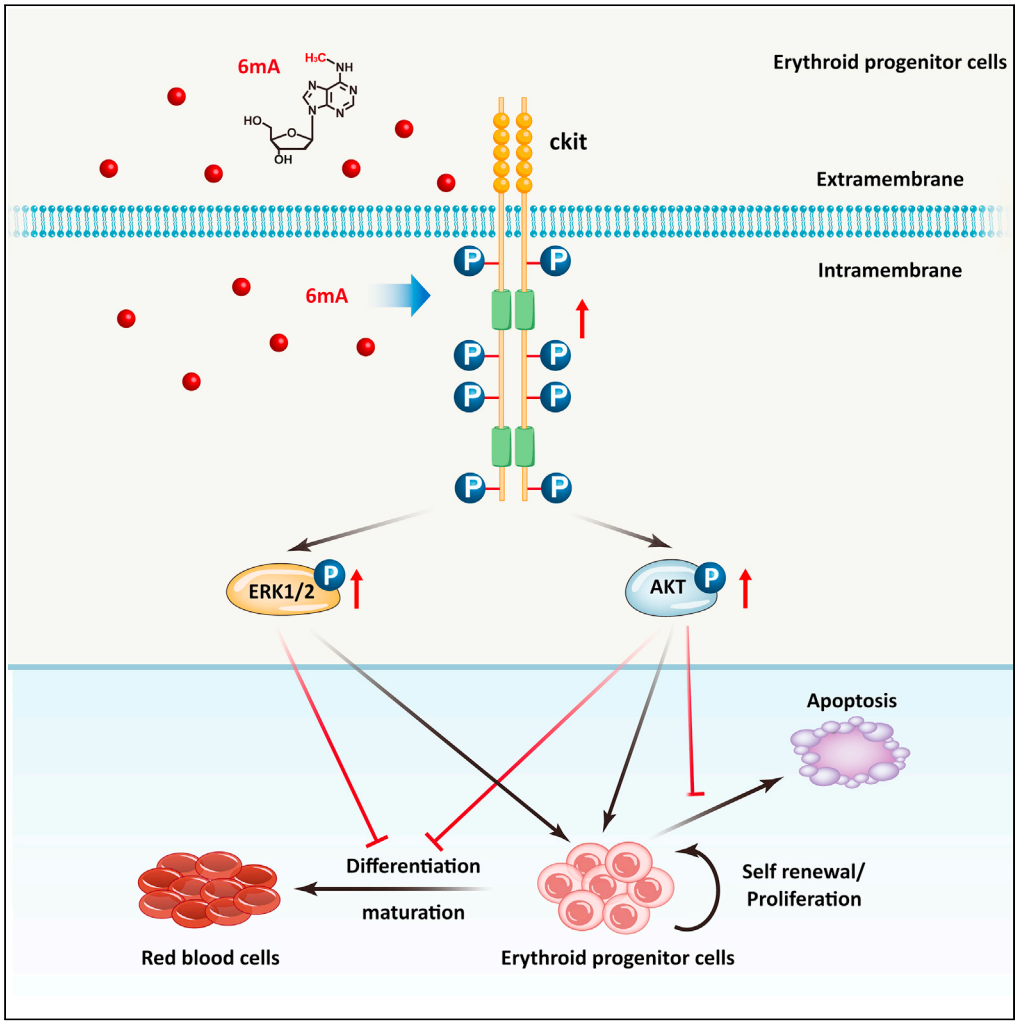

Yao Li, Zi-Yu Liang, Hai-Lin Wang

hlwang@rcees.ac.cn

Highlights

6mdA stimulates self-renewal of BFU-E progenitor

6mdA enhances and prolongs the activation of c-Kit signaling pathways

6mdA enhances the activation of c-Kit downstream MAPK/ERK and PI3K-AKT pathways

Li et al., iScience 26, 106924
June 16, 2023 © 2023 The Author(s).
https://doi.org/10.1016/j.isci.2023.106924

iScience

CellPress
OPEN ACCESS

Article

N6-methyl-2′-deoxyadenosine promotes self-renewal of BFU-E progenitor in erythropoiesis

Yao Li,[1,2] Zi-Yu Liang,[1,2] and Hai-Lin Wang[1,2,3,4,*]

SUMMARY

Red blood cells supply the oxygen required for all human cells and are in demand for emerging blood-loss therapy. Here we identified N6-methyl-2′-deoxyadenosine (6mdA) as an agonist that promotes the hyperproliferation of burst-forming unit erythroid (BFU-E) progenitor cells. In addition, 6mdA represses the apoptosis of erythroid progenitor cells (EPCs). Combined use of with SCF and EPO enabled cultures of isolated BFU-E to be expanded up to 5,000-fold. Transcriptome analysis showed that 6mdA upregulates the expression of the EPC-associated factors c-Kit, Myb, and Gata2 and downregulates that of the erythroid maturation-related transcription factors Gata1, Spi1, and Klf1. Mechanistic studies suggested that 6mdA enhances and prolongs the activation of erythropoiesis-associated master gene c-Kit and its downstream signaling, leading to expansion and accumulation of EPCs. Collectively, we demonstrate that 6mdA can efficiently stimulate the EPC hyperproliferation and provide a new regenerative medicine recipe to improve *ex vivo* generation of red blood cells.

INTRODUCTION

Blood transfusion is a common therapeutic modality for chronic anemia[1] and provides important support for other clinical therapies.[2] Nevertheless, supply shortages, the transmission of blood-borne pathogens and the overall costs of the process have promoted many efforts to search for alternative transfusion sources. *Ex vivo* generation of red blood cells via erythropoiesis has been proposed as a promising strategy to ensure an adequate and safe supply of blood cell products. For this purpose, a few types of stem/progenitor cells are potentially useful for the generation of red blood cells, including human embryonic stem cells,[3,4] umbilical cord blood cells,[5] adult peripheral blood $CD34^+$ cells,[6,7] and induced pluripotent stem cells.[8] The existing bioengineering methods for *ex vivo* preparation of red blood cells all require undergoing the stages of erythroid progenitor cells (EPCs), after which the EPCs are induced to differentiate into mature red blood cells. Therefore, EPC proliferation is essential for *ex vivo* preparation of red blood cell preparation.

Erythropoiesis is a multiple-step process of transition from hematopoietic stem cells to red blood cells. It can be divided into two stages: early-stage erythropoiesis and terminal erythroid differentiation.[9] Burst-forming unit erythroid (BFU-E) cells are the first committed EPCs generated from hematopoietic stem cells. BFU-E cells are then differentiated into late erythroid progenitor colony-forming unit erythroid (CFU-E) cells and proerythroblasts. Proerythroblasts enter terminal erythroid differentiation to form basophilic erythroblasts, polychromatic erythroblasts, and orthochromatic erythroblasts and finally expel the nuclei to form mature red blood cells in mammals.[10]

Two protein factors, stem cell factor (SCF)[11] and erythropoietin (EPO),[12] have been found to stimulate the growth and proliferation of EPCs. They play essential roles in erythroid development and are commonly used cytokines during *ex vivo* culture of EPCs. The binding of the dimeric SCF molecule to its specific receptor c-Kit induces c-Kit dimerization of and intermolecular autophosphorylation, leading to the activation of c-Kit kinase.[13] Then, phosphorylated c-Kit activates downstream signaling pathways, such as the phosphatidylinositide-3′-kinase (PI3K)/protein kinase B (AKT) and mitogen-activated protein kinase (MAPK)/extracellular signal-regulated kinase (ERK) signaling pathways to regulate proliferation.[11,14] During erythropoiesis, c-Kit functions as a master gene and regulates the survival, expansion, and differentiation of EPCs.[15,16] c-Kit-deficient mice exhibit a severe reduction in CFU-E progenitors and die of anemia around day 16 of gestation.[11] On the other hand, c-Kit activating mutations of human erythroblasts are

[1]State Key Laboratory of Environmental Chemistry and Ecotoxicology, Research Center for Eco-Environmental Sciences, Chinese Academy of Sciences, Beijing 100085, China

[2]University of Chinese Academy of Sciences, Beijing 100049, China

[3]Institute of Environment and Health, Jianghan University, Wuhan, Hubei 430056, China

[4]Lead contact

*Correspondence: hlwang@rcees.ac.cn

https://doi.org/10.1016/j.isci.2023.106924

This is an open access article under the CC BY-NC-ND license (http://creativecommons.org/licenses/by-nc-nd/4.0/).

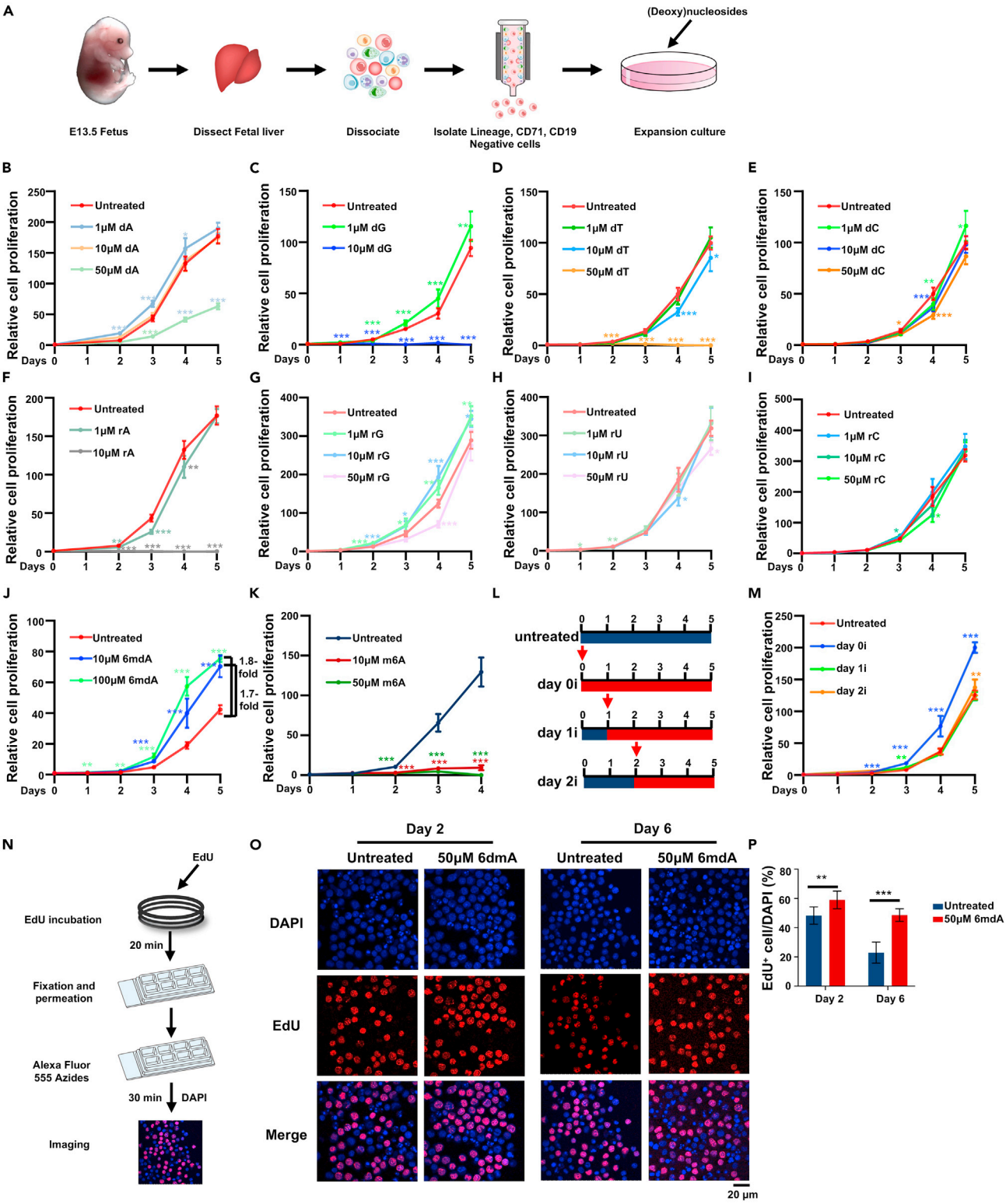

Figure 1. Effect of (deoxy)nucleosides on proliferation of EPCs

(A) Schematic of EPC sorting.

(B) Relative cell proliferation of EPCs after dA, (C) dG, (D) dT, (E) dC, (F) rA, (G) rG, (H) rU, (I) rC, (J) 6mdA and (K) m6A treatment was analyzed by MTS. Each treatment contained six technical replicates.

Figure 1. *Continued*

(L) Schematic diagram of different 6mdA treatment times (the red arrow represents the time when 6mdA was added), "i" means "input".

(M) Cell proliferation was monitored after 6mdA nucleoside treatment at different times. Each treatment contained six technical replicates.

(N) Schematic of EdU incorporation detection.

(O) Images of cell proliferation analysis by EdU incorporation.

(P) Mean and SD of the percentage of EdU-positive (EdU^+) EPCs with or without 6mdA treatment. Each treatment contained five to ten replicates. The p values in 1B-1K and 1M were calculated by one-way ANOVA. The p values in 1P were calculated by unpaired t.test (no significance is not shown, *p<0.05, **p<0.01, ***p<0.001).

capable of robust expansion *ex vivo*.[17] EPO at low concentrations facilitates the proliferation of EPCs by activating the PI3K and Shc/Ras pathways, whereas EPO-induced terminal differentiation appears to be mainly associated with the activation of signal transducer and activator of transcription 5 (STAT5).[18]

The glucocorticoid receptor (GR) agonist dexamethasone has also been shown to stimulate the proliferation of BFU-E cells by enhancing the activation of HIF1α. Moreover, the combination of dexamethasone and the prolyl hydroxylase inhibitor (PHI) DMOG greatly enhances the proliferation of BFU-E cells, leading to a 3.8-fold increase over that achieved with dexamethasone alone.[19]

To date, the challenge in *ex vivo* culture of EPCs is still the limit of their proliferation capacity. The expression and activation of c-Kit are key to the proliferation of EPCs. However, c-Kit is soon downregulated to permit subsequent maturation.[20] Such transient c-Kit activation limits the proliferation or self-renewal capacity of EPCs. Genetic manipulation (persistent c-Kit activation) may enhance proliferation but affect terminal differentiation.[17]

Here, we unexpectedly discovered that 2′-deoxynucleoside 6mdA can stimulate the proliferation of BFU-E cells by upregulating and activating c-Kit. We showed that the activation of c-Kit by 6mdA further activates the ERK/MAPK and PI3K/AKT signaling pathways. Based on this finding, we developed a recipe for *ex vivo* generation of red blood cells.

RESULTS

2′-deoxynucleoside 6mdA stimulates the hyperproliferation of EPCs

Nucleosides have been reported to modulate cell proliferation, differentiation, and death in normal cells[21,22] and leukemic cells.[23] In particular, adenosine has been shown to stimulate erythropoietin production in erythropoiesis of the plethoric mouse.[24] To explore the effects of nucleosides on the proliferation of EPCs, we isolated EPCs from E13.5 fetal livers based on a previous protocol (Figure 1A).[25] Using these *ex vivo* cultured cells, we tested 10 (deoxy)nucleosides (Figure S1). Among these (deoxy)nucleosides, we observed that during *ex vivo* culture, five (deoxy)nucleosides severely inhibited the proliferation of EPCs, four did not affect the proliferation, and only one increased proliferation. Specifically, 2′-deoxyadenosine (dA) at 50 μM and N6-methyladenosine (m6A) at 10 μM inhibited proliferation by 65% and 94% (Figures 1B and 1K), respectively. The observation that m6A repressed erythropoiesis is consistent with previous literature.[26] 2′-Deoxythymidine (dT) at 50 μM, adenosine (rA) at 10 μM, and 2′-deoxyguanosine (dG) at 10 μM completely blocked proliferation (Figures 1C, 1D, and 1F). 2′-Deoxycytidine (dC), cytidine (rC), uridine (rU) and guanosine (rG) had no notable effect on proliferation at concentrations of 1.0–50 μM (Figures 1E and 1G–1I). Of interest, only N6-methyl-2′-deoxyadenosine (6mdA) stimulated the proliferation of EPCs (Figure 1J).

To further explore whether 6mdA-induced proliferation only existed in the early stage or throughout the whole culture period, we treated cells with 6mdA on different expansion days (Figure 1L). Treatment started at day 0 increased the proliferation of EPCs. However, 6mdA treatment started with a one- or two-day delay failed to increase proliferation (Figure 1M).

To further validate whether 6mdA increases the proliferation ability of EPCs, we used 5-ethynyl-2′-deoxyuridine (EdU) to evaluate proliferation (Figure 1N). Immunofluorescence imaging of EdU revealed that EPCs had high proliferative capacity (~70%) in the first two days of culture regardless of 6mdA treatment. This was consistent with the results obtained using the luminescence proliferation assay (Figure 1O). However, when we tested the proliferation capacity on the sixth expansion day, the proportion of EdU^+ cells in the 6mdA-treated group were reduced from 70% to 56%, whereas that in the untreated group was reduced from 60% to 32% (Figure 1P). Consistently, EdU incorporation analyzed by flow cytometry showed that

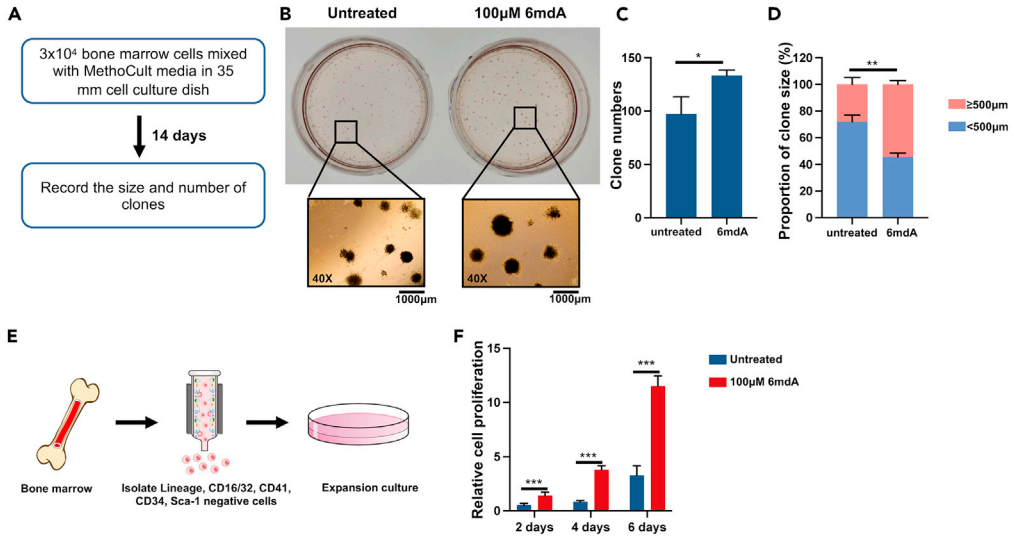

Figure 2. 6mdA promote the proliferation of BMC-derived progenitor cells

(A) Flow chart of the BFU-E colony formation assay.

(B) Visual images of BMC derived BFU-E clones with or without 6mdA treatment.

(C) BMC derived BFU-E clone numbers with or without 6mdA treatment. Each treatment had three biological replicates.

(D) The proportion of BFU-E clone size, divided by 500 μm in diameter. Each treatment contained three biological replicates.

(E) Schematic of sorting a mix of BFU-E and CFU-E cells from BMC.

(F) MTS cell proliferation assay of a mix of BFU-E and CFU-E cells derived from BMCs. Each treatment had six technical replicates. Data are presented as mean ± SD. The p values were calculated by unpaired t.test (N. S., no significance, *p<0.05, **p<0.01, ***p<0.001).

6mdA treatment increased the percentage of proliferative cells of EPCs after expansion 4-, 6-, or 8 days (Figure S2).

We further investigated the effect of 6mdA on adult bone marrow derived EPCs. For this purpose, we performed a BFU-E colony assay on bone marrow cells (BMCs) (Figure 2A). We observed that 6mdA treatment increased the colony number significantly (Figures 2B and 2C). In addition, the colony size for the 6mdA-treated group was larger than that for the untreated group. Specifically, more than 50% of the clones were 500 μm or greater in diameter for 6mdA treatment, whereas only 24% of the clones were 500 μm or greater in diameter for the untreated group (Figure 2D). Referring to the method for isolating a pure mix of BFU-E and CFU-E cells from fetal liver cells,[19] we sorted a mix of BFU-E and CFU-E cells from adult mouse bone marrow by removing lineage panel (Ter119, CD3ε, CD11b, Gr1, and CD45R), CD16/32, CD41, CD34 and Sca-1 positive cells (Figure 2E). 6mdA treatment clearly increased the proliferation of the sorted cells. After 4 days of expansion culture, 6mdA treatment group showed a 4-fold increase of cell proliferation, whereas in the 6mdA-absent untreated group, cells barely grew. (Figure 2F).

These results indicated that 6mdA treatment stimulates the EPCs to maintain their proliferation ability over longer *ex vivo* culture.

2′-deoxynucleoside 6mdA upregulates and activates the erythropoiesis-essential receptor tyrosine kinase c-Kit

We next wondered how 6mdA stimulates the proliferation of EPCs. To answer this question, we used next-generation sequencing to evaluate the differential gene expression of individual messenger RNAs (mRNAs) in 4 days of culture with or without 6mdA nucleoside. A total of 1789 protein-coding genes were significantly altered on 100 μM 6mdA treatment. Among these genes, we found that the expression of erythropoiesis-essential receptor tyrosine kinase c-Kit was upregulated (Figure 3A). In addition, Myb and Gata2, two important transcription factors in maintaining the proliferative state and promoting the proliferation of hematopoietic progenitor cells, including EPCs,[27,28] were upregulated. In contrast, the levels of several genes expressed at late stages of EPC differentiation, including two primary enzymes in heme

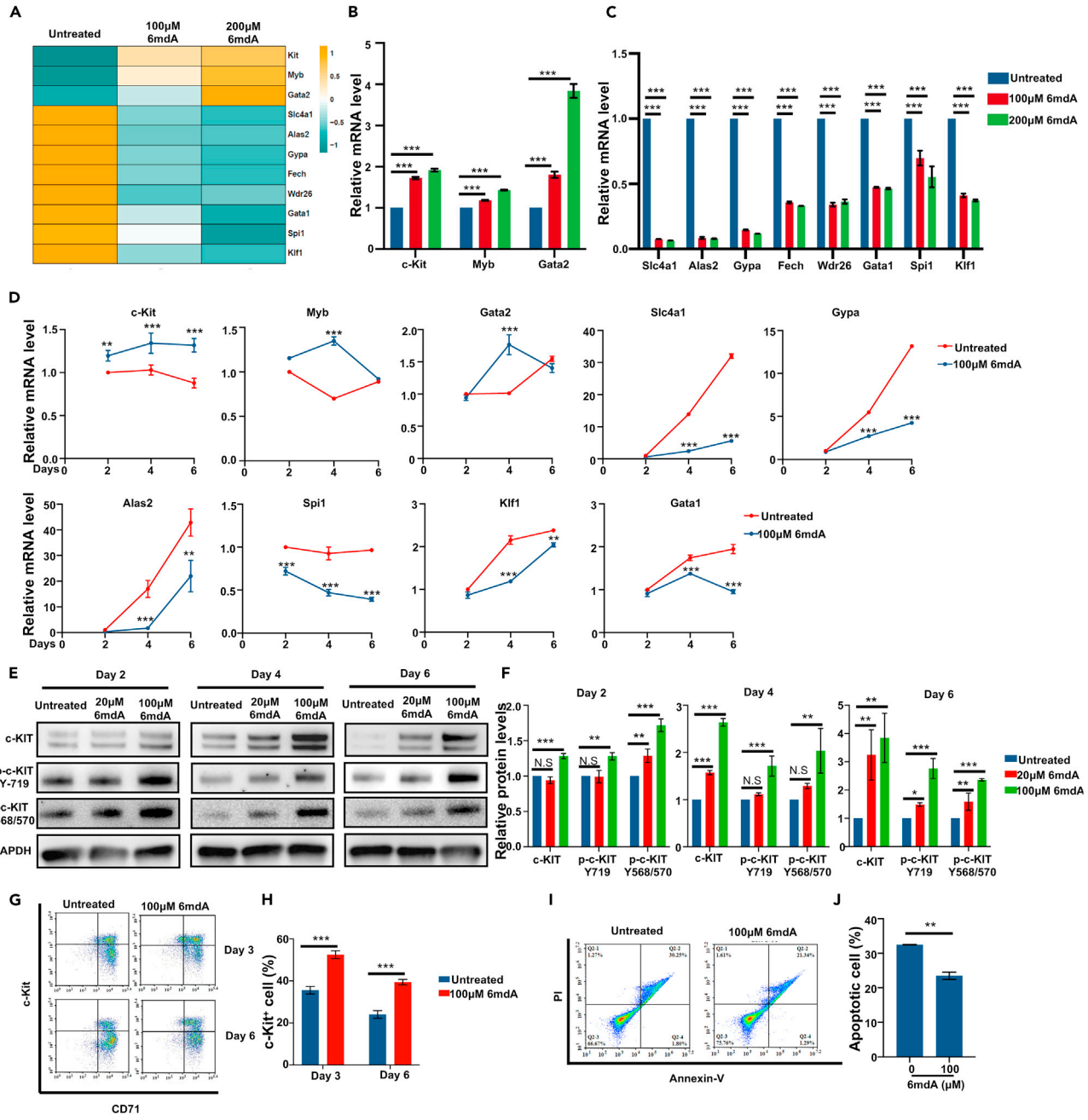

Figure 3. 6mdA upregulates and activates c-Kit

(A) Heatmap of the genes involved in the proliferation and differentiation of erythroid progenitors.

(B) mRNA levels of c-Kit, Myb, Gata2 and (C) Slc4a1, Alas2, Gypa, Fech, Wdr26, Gata1 Spi1 and Klf1 as revealed by RT-qPCR. Each treatment contained three replicates.

(D) The dynamic expression of c-Kit, Myb, Gata2, Slc4a1, Alas2, Gypa, Gata1 Spi1 and Klf1 on the indicated expansion days was determined by q-PCR. The relative expression normalized to GAPDH was shown. Each treatment contained three replicates.

(E) Western blot analysis of the expression and phosphorylation of c-Kit on the indicated days in EPCs.

(F) Quantitative analysis of the expression and phosphorylation of c-Kit from 3 independent experiments of EPCs.

(G) c-Kit$^+$ cells according to the surface expression of c-Kit and CD71 culture on the indicated days of EPCs. (H) Quantitative analysis of c-Kit$^+$ cells from three independent experiments of EPCs. (I) Flow cytometry analysis of EPCs apoptosis after 6 days of expansion.

(J) Quantitative analysis of apoptotic cells of EPCs from three independent experiments. Data are presented as mean ± SD. The p values in 3B-3C and 3F were calculated by one-way ANOVA. The p values in 3D, 3H and 3J were calculated by unpaired t.test (N. S., no significance, *p<0.05, **p<0.01, ***p<0.001).

biosynthesis (5-aminolevulinate synthase 2 (Alas2), ferrochelatase (Fech)), one important protein for promoting nuclear condensation (WD40 repeat protein 26 (Wdr26)), red blood cell anion exchanger solute carrier family 4 member 1 (Slc4a1) and glycophorin A (Gypa)[29–32] were lower than those in the untreated group. The expression levels of the transcription factors Gata1, Spi1 and Klf1,[33–35] which establish the onset and progression of terminal differentiation events, were also downregulated after 6mdA treatment (Figure 3A). The elevations in the mRNA expression of three proliferation-associated genes (c-Kit, Myb and Gata2) (Figure 3B) and the reduced levels of mRNA expression of eight differentiation-related genes (Slc4a1, Alas2, Gypa, Fech, Wdr26, Gata1, Spi1 and Klf1) (Figure 3C) were further validated by quantitative reverse-transcription PCR (RT-qPCR) analysis. We also showed the dynamic expression of these genes during the indicated expansion days (days 2, 4, and 6). These results showed that 6mdA treatment upregulated the expression of c-Kit and retarded the upregulation of differentiation-related genes, including Slc4a1, Alas2, Gypa, Gata1, Spi1 and Klf1 (Figure 3D).

We next examined the protein expression of the tyrosine kinase receptor c-Kit, which is a pivotal protein supporting the proliferation of EPCs. Consistent with the increase in the mRNA level, the protein level of c-Kit also increased after treatment with 100 μM 6mdA (approximately 1.2-fold, 2.6-fold, and 3.8-fold in expansion of 2, 4 and 6 days, respectively) compared to that for the untreated control group (Figures 3E and 3F).

Moreover, we examined two phosphorylated sites of c-Kit (Tyr568/570 and Tyr719) that are associated with the activation of MAPK/ERK and PI3K/AKT, respectively.[36–39] Western blot analysis showed that both phosphorylated Tyr568/570 and Tyr719 of c-Kit increased. Specifically, Tyr568/570 phosphorylation of c-Kit increased by approximately 1.7-fold, 2-fold, and 2.4-fold after 2, 4, and 6 days of expansion, and Tyr719 phosphorylation of c-Kit increased by approximately 1.2-fold, 1.7-fold, and 2.7-fold after 2, 4 and 6 days of expansion (Figures 3E and 3F). The results suggest that, on c-Kit activation, MAPK and PI3K might also be activated.

6mdA retards differentiation and preserves EPCs

Because c-Kit is expressed as a marker only in early EPCs, including BFU-E and CFU-E,[20] we examined the proportion of c-Kit$^+$ cells by monitoring the surface expression of c-Kit. Flow cytometry analysis of the sorted EPCs (marked by high c-Kit and CD71$^+$) cultured for different periods of time showed that 6mdA treatment prolonged the proliferation of early EPCs and retarded the differentiation, approximately 40% remained c-Kit$^+$ after 6 days of expansion with 100 μM 6mdA treatment compared with 24% in the untreated group (Figures 3G and 3H). Furthermore, flow cytometry analysis of EPCs stained with propidium iodide/annexin V revealed that 6mdA treatment reduced apoptosis from 32% to 22% after 6-day expansion (Figures 3I and 3J). These results suggest that 6mdA treatment effectively preserves EPCs during 6-day expansion by retarding the differentiation and reducing the apoptosis of EPCs, thus promotes the proliferation of EPCs.

6mdA activates c-Kit downstream pathways

c-Kit participates in important cellular signal transduction processes through different intracellular signaling pathways, including the PI3K/AKT and MAPK/ERK signaling pathways (Figure 4A). To investigate whether 6mdA-induced c-Kit activation can also cause MAPK/ERK and PI3K/AKT pathway activation, we examined the phosphorylation levels of the important downstream proteins ERK1/2 and AKT. As shown in Figure 4B, after 6mdA treatment, the expression of ERK1/2 was not notably altered, but the phosphorylation of ERK1/2 was significantly increased in EPCs cultured for the indicated days (Figure 4B). After 100 μM 6mdA treatment, the phosphorylation level of ERK1/2 was increased 3-fold and 4.3-fold after expansion for 2 and 6 days, respectively (Figure 4C). As treated with 100 μM 6mdA, the phosphorylation level of AKT was increased 2-fold, 3.7-fold and 2.6-fold in EPCs after expansion for 2, 4 and 6 days, respectively, whereas the expression of AKT was not altered (Figures 4D and 4E). We also examined EPO-induced STAT5 activation. However, the expression of STAT5 was not altered in EPCs. The phosphorylation of STAT5 was not changed after 2 days of culture and decreased to 60% after 4 and 6 days of culture with 100 μM 6mdA treatment (Figure S3). Collectively, these findings indicated that 6mdA treatment activated the two c-Kit downstream signaling pathways, MAPK/ERK and PI3K/AKT, in EPCs.

Initial observations showed that 6mdA enhanced the proliferation of EPCs only when 6mdA was added on day 0 (Figure 1M). We measured the levels of p-c-Kit, *p*-ERK and *p*-AKT using western blot (Figure S4). Evidently, the expression and phosphorylation levels of c-Kit were elevated only when the EPCs were

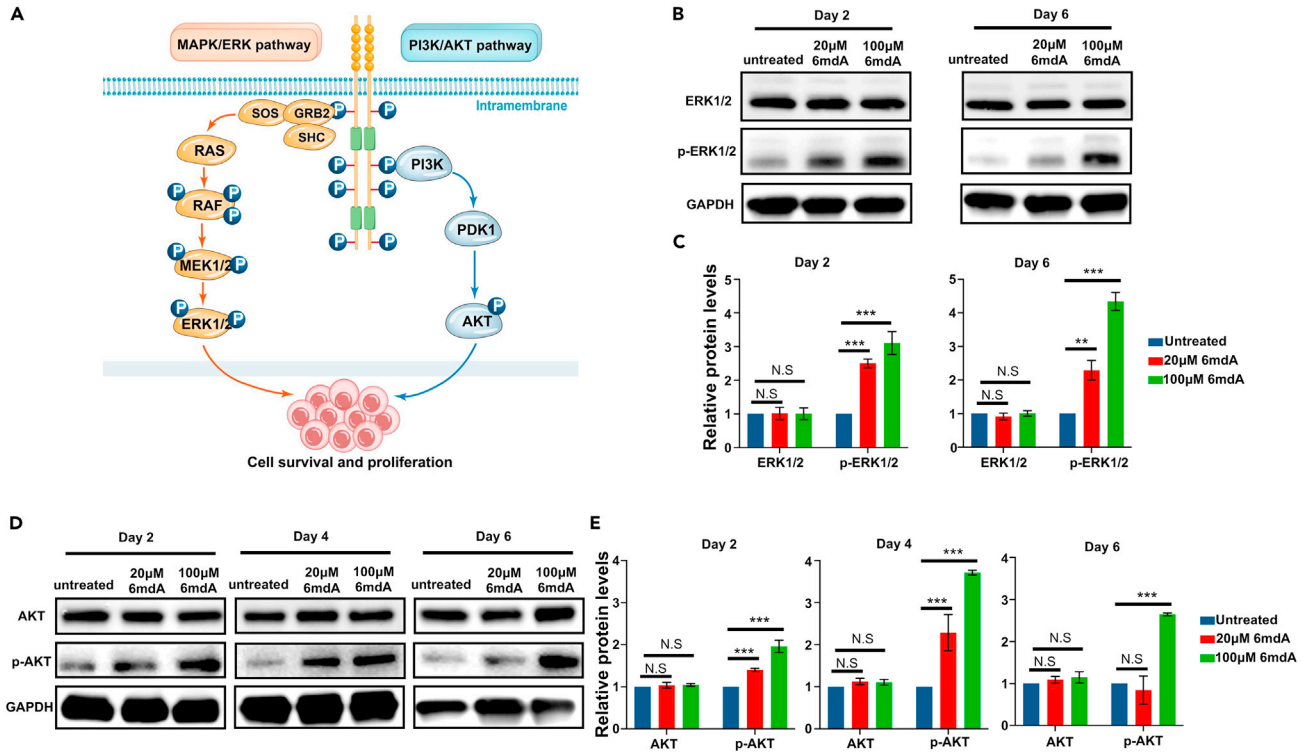

Figure 4. 6mdA exposure led to activation of the signaling pathway downstream of c-Kit

(A) Schematic diagram of the signaling pathways downstream of c-Kit.

(B) Western blot analysis of the expression and phosphorylation of ERK1/2 and (D) AKT in EPCs on the indicated days.

(C) Quantitative analysis of the expression and phosphorylation of ERK1/2 and (E) AKT protein levels from three independent experiments of EPCs. Data are presented as mean ± SD. The p values were calculated by one-way ANOVA (N.S., no significance, *p<0.05, **p<0.01, ***p<0.001).

treated with 6mdA from day 0 (3.5-fold increase in expression level and 2.6-fold increase in phosphorylation) (Figures S4A and S4D). Consistently, the phosphorylation of ERK1/2 and AKT showed the most significant increase when the treatment of EPCs with 6mdA started from day 0 (1.5-fold and 1.7-fold increases in phosphorylation of ERK1/2 and AKT, respectively) (Figures S4B, S4C, S4E, and S4F). These results further demonstrated that the proliferation of EPCs can be promoted only when c-Kit activation is increased.

6mdA antagonizes c-Kit inhibition

Treating EPCs with the c-Kit inhibitor STI571 (10 nM, 50 nM and 100 nM) showed a dose-dependent inhibition on proliferation. The treatment with 10 nM STI571 had little effect on cell proliferation, but treatment with 50 nM and 100 nM STI571 dramatically inhibited the growth of EPCs (Figures 5A–5C). This is in agreement with previous literature.[9] Of interest, 6mdA treatment mitigated the STI571-induced inhibition of EPC proliferation. 6mdA increased the proliferation of EPCs by approximately 3-fold in the 10 nM STI571 treatment group and increased it by 10-fold in the 50 nM STI571 treatment group (Figures 5A and 5B). Consistently, western blot analysis showed that, as treated with 10 nM and 50 nM STI571, 6mdA still increased the expression and phosphorylation of c-Kit (Figures 5D and 5E). However, it was difficult to induce cell proliferation after 100 nM STI571 inhibition (Figure 5C). Western blot analysis showed that after STI571 inhibition at 100 nM, 6mdA hardly increased the phosphorylation of c-Kit (Figure 5F).

The specific ligand SCF binds to c-Kit inducing receptor activation and signal transduction.[40] SCF deficiency depletes hematopoietic progenitors, including EPCs.[41] Thus, the relative cell proliferation of the cells cultured in medium supplemented with SCF at different concentrations was measured. In agreement with STI571 inhibition, when the concentration of SCF decreased to 10 ng/mL, the proliferation of EPCs was severely inhibited, whereas 6mdA could elevate the cell proliferation (Figure 5G). However, the absence of SCF caused severe proliferation inhibition of EPCs. Concomitantly, 6mdA failed to induce hyperproliferation (Figure 5H).

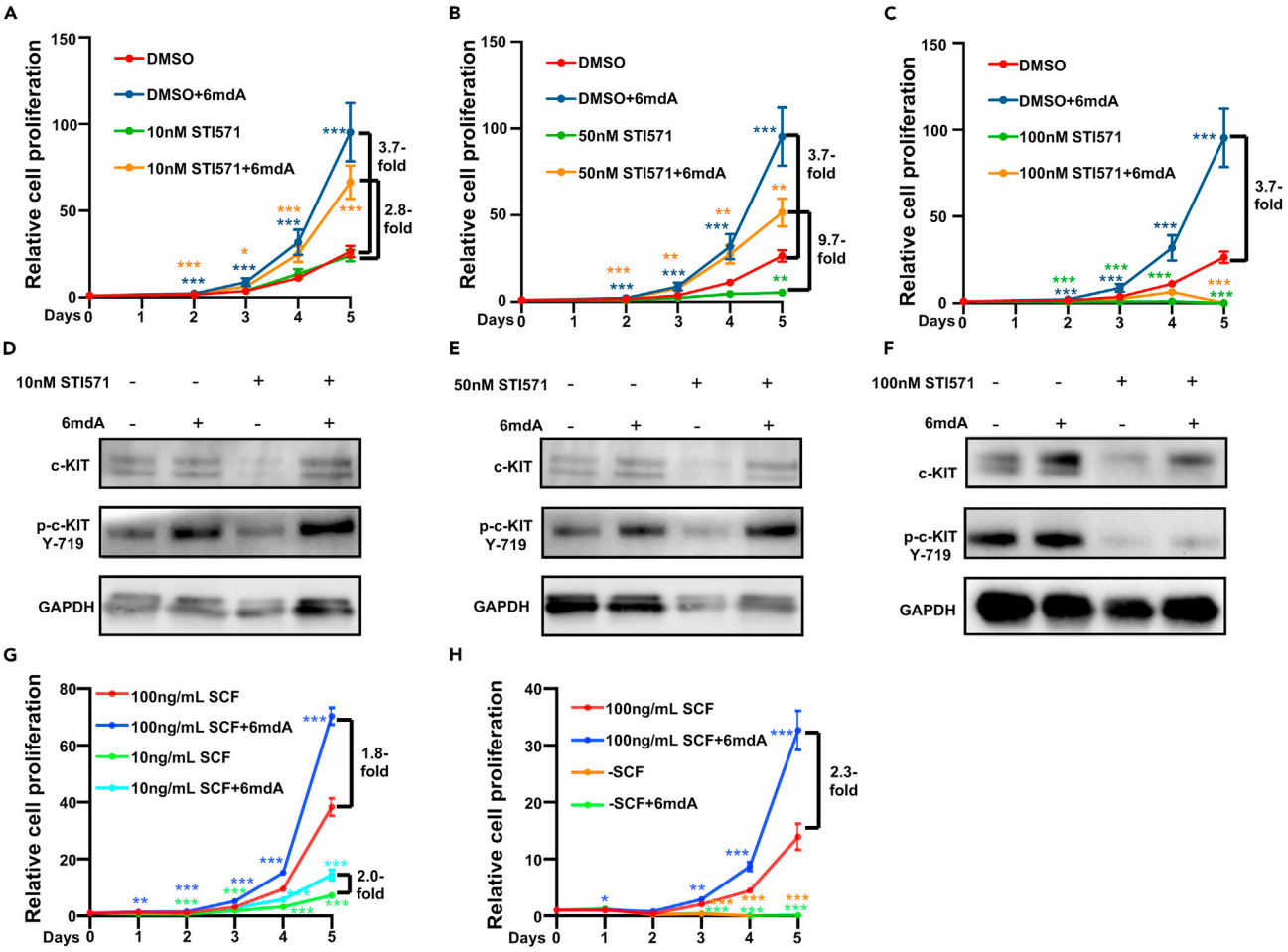

Figure 5. 6mdA antagonizes c-Kit inhibition

(A) Cell proliferation analysis after treatment with 10 nM, (B) 50 nM, and (C) 100 nM STI571 by MTS. Each treatment contained six technical replicates.

(D) Western blot analysis of the expression and phosphorylation of c-Kit after treatment with 10 nM, (E) 50 nM, and (F) 100 nM STI571.

(G) Cell proliferation analysis of EPCs cultured with 100 ng/mL or 10 ng/mL SCF by MTS. Each treatment contained six technical replicates.

(H) Cell proliferation analysis of EPCs cultured with 100 ng/mL or no SCF by MTS. Each treatment contained six technical replicates. Data are presented as mean ± SD. The p values were calculated by one-way ANOVA (no significance was not shown, *p<0.05, **p<0.01, ***p<0.001).

The above results indicate that 6mdA treatment has an antagonistic effect on c-Kit inhibition. On the other hand, these data also consistently support the idea that 6mdA-induced proliferation is associated with c-Kit activation.

To further investigate whether ERK1/2 and AKT activation is associated with 6mdA-induced hyperproliferation, we examined the proliferation of EPCs in the presence of the MAPK/ERK pathway inhibitors selumetinib and U0126. After treatment with 1 μM selumetinib or 1 μM U0126, the phosphorylation of ERK1/2 was significantly inhibited (Figures S5D and S5E). The proliferation of EPCs was also significantly inhibited (Figures S5A and S5B). However, 6mdA also mitigated the inhibition of EPC proliferation (Figures S5A and S5B). Similarly, after the phosphorylation of AKT was inhibited by treatment with the PI3K/AKT inhibitor LY294002 (Figures S6 and 5F), the proliferation of EPCs was also inhibited, but 6mdA partly mitigated this inhibition and increased the proliferation (Figure S5C).

6mdA mainly induces hyperproliferation of BFU-E cells

Initial observations that only 6mdA treatment started from day 0 could enhance the proliferation of EPCs (Figure 1M) led us to hypothesize that the proliferation of BFU-E cells, but not CFU-E cells, are enhanced by 6mdA. To further investigate the cell population on which 6mdA acted, we sorted early erythroid

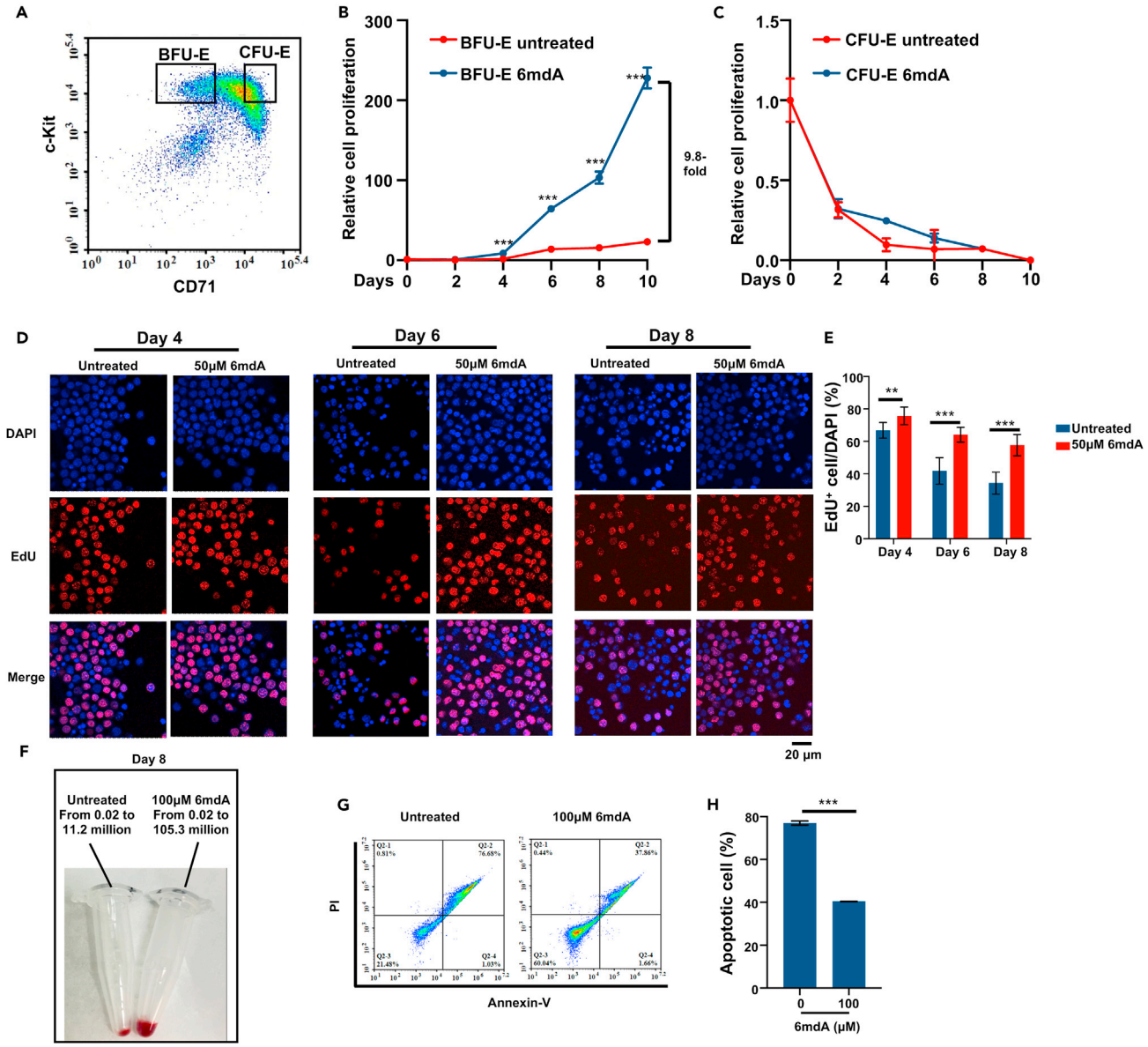

Figure 6. 6mdA promotes the proliferation of BFU-E cells

(A) BFU-E and CFU-E cell sorting by flow cytometry according to the expression of CD71 and c-Kit, c-Kit^{+}CD71$^{10\%low}$ represents BFU-E, and c-Kit^{+}CD71$^{20\%high}$ represents CFU-E.

(B) Relative cell proliferation of BFU-E and (C) CFU-E after 6mdA treatment were analyzed by MTS. Each treatment contained six technical replicates.

(D) Images of cell proliferation analysis by EdU incorporation of BFU-E cells.

(E) Mean and SD of the percentage of EdU-positive (EdU^{+}) BFU-E cells with or without 6mdA treatment. Each treatment contained five to ten replicates.

(F) Visual images of BFU-E cells after expansion for 8 days with or without 6mdA treatment.

(G) Flow cytometry analysis of the apoptosis of BFU-E cells after 6 days expansion.

(H) Quantitative analysis of apoptotic cells of BFU-E cells from three independent experiments. Data are presented as mean ± SD. The p values were calculated by unpaired t test (*p<0.05, **p<0.01, ***p<0.001).

progenitor BFU-E and CFU-E cells from EPCs. After magnetic depletion of mouse lineage panel (Ter119, CD3ε, CD11b, Gr1, and CD45R), CD16/CD32, Sca-1, CD34, and CD41 positive cells from fetal liver cells, BFU-E and CFU-E cells were sorted from the Kit^{+} fractions according to the expression level of CD71 by flow cytometry. The BFU-E fraction had the 10% lowest CD71 expression (CD71$^{10\%low}$), and the CFU-E fraction had the 20% highest CD71expression (CD71$^{20\%high}$) (Figure 6A).[19]

As stimulated by 6mdA (100 μM), BFU-E displayed increased proliferation (Figure 6B). Although there was no significant difference in the BFU-E cell proliferation during the first 2 days, adding 6mdA resulted in an approximately 10-fold increase in cell proliferation compared with that in the untreated group after 10 days of expansion (Figure 6B). EdU incorporation analysis also showed that 6mdA increased the proliferation of BFU-E cells (Figure 6D). After 8 days of culture, approximately 60% of BFU-E cells had high proliferative ability after 6mdA treatment, whereas only 40% of BFU-E cells still had proliferation capacity in the untreated group (Figure 6E). Flow cytometry analysis of EdU incorporation also showed a 1.5-fold increase in the proliferation ability of BFU-E cells after 6mdA treatment (represented by the proportion of EdU^+ cells) (Figure S6). In contrast, 6mdA treatment failed to promote CFU-E proliferation (Figure 6C). To provide direct visual evidence, we collected BFU-E cells after 8 days of expansion, and visual images showed an approximately 10-fold increase in cell number after 6mdA treatment. Combined treatment with SCF and EPO enabled cultures of purified BFU-E with 6mdA to be expanded up to 5,000-folds (from 0.02 million to 11 million in the untreated group compared with 0.02 million to 105 million in the 100 μM 6mdA treatment group) (Figure 6F). In addition, the apoptosis of cultured BFU-E cells was partly blocked by 6mdA treatment, and the percentage of apoptotic cells was reduced from 77% to 40% (Figures 6G and 6H). Collectively, these results show that 6mdA mainly stimulates the proliferation and impairs the apoptosis of BFU-E cells.

6mdA activates c-Kit and its downstream signaling pathways in BFU-E cells

To verify that the regulatory mechanism of 6mdA stimulates the proliferation of BFU-E cells, we performed next-generation sequencing to determine the differential expression of individual messenger RNAs (mRNAs) in 6-day-cultured BFU-E cells in the presence or absence of 6mdA. Consistently, 6mdA treatment upregulated the expression of the erythroid progenitor-associated genes c-Kit, Myb and Gata2, and downregulated the expression of the differentiation-related genes Slc4a1, Alas2, Gypa, Wdr26, Spi1, Klf1, Gata1 and Fech (Figure 7A). These results were further validated by RT-qPCR (Figures 7B and 7C).

Consistent with the effect on EPCs, we also hypothesized that 6mdA activates c-Kit and its downstream pathways. To test this hypothesis, the $c\text{-}Kit^+$ population was monitored after expansion of BFU-E cells for 3 and 6 days. After 3 days of expansion, most of BFU-E cells carried high abundance of surface c-Kit+ (>70%). However, approximately 35% of the cells remained $c\text{-}Kit^+$ after 6 days of expansion with 100 μM 6mdA treatment, whereas only approximately 14% were $c\text{-}Kit^+$ in the untreated group (Figures S7A and S7C), indicating that 6mdA treatment prolonged the accumulation of BFU-E cells. When EPCs enter terminal differentiation after proerythroblasts, the expression of Ter119 is gained.[10] Based on the expression of CD71 and Ter119, the differentiation of BFU-E cells was analyzed. We first validated that 6mdA was evaluated the proliferation of BFU-E cells after 3 or 6 days of expansion culture (Figures S7B and S7D). Flow cytometry analysis showed that the differentiation of BFU-E cells was retarded by 6mdA treatment after 3 days of expansion, 15% of the cells expressed Ter119 after expansion 6 days in untreated group, whereas only 10% of cells were $Ter119^+$ in 6mdA-treated group (Figure S7A). While after 6 days of expansion, 35% of the cells expressed Ter119 after expansion 6 days in untreated group, 44% of cells were $Ter119^+$ in 6mdA-treated group (Figure S7C). These results suggested that the 6mdA-enhanced proliferation is not simply attributed to the 6mdA-induced differentiation inhibition. Furthermore, western blot analysis showed that the expression and phosphorylation of c-Kit were also elevated in BFU-E cells as stimulated by 6mdA (approximately 4-fold increase in expression and 2-fold increase in phosphorylation) (Figures 7D and 7E).

On shRNA-mediated knockdown of c-Kit in BFU-E cells (40% knockdown, Figure 7F), the proliferation ability of BFU-E cells was significantly decreased, concomitantly 6mdA-induced proliferation of BFU-E cells was compromised (Figure 7G). These results indicated that the c-Kit signaling pathway plays an important role in 6mdA-induced hyperproliferation of BFU-E cells.

Consistent with the observation for EPCs, the phosphorylation of ERK1/2 and AKT was also elevated after 6mdA treatment in BFU-E cells by 2.6- and 2.7-fold, respectively (Figures 7H–7K).

6mdA does not impair the differentiation of erythroid progenitors

6mdA treatment during *ex vivo* expansion enabled more EPCs to be obtained. To explore whether 6mdA-induced hyperproliferated EPCs could proceed to differentiate and mature normally, we cultured EPCs with 6mdA during the expansion phase for 3 days and then withdrew the 6mdA treatment and induced

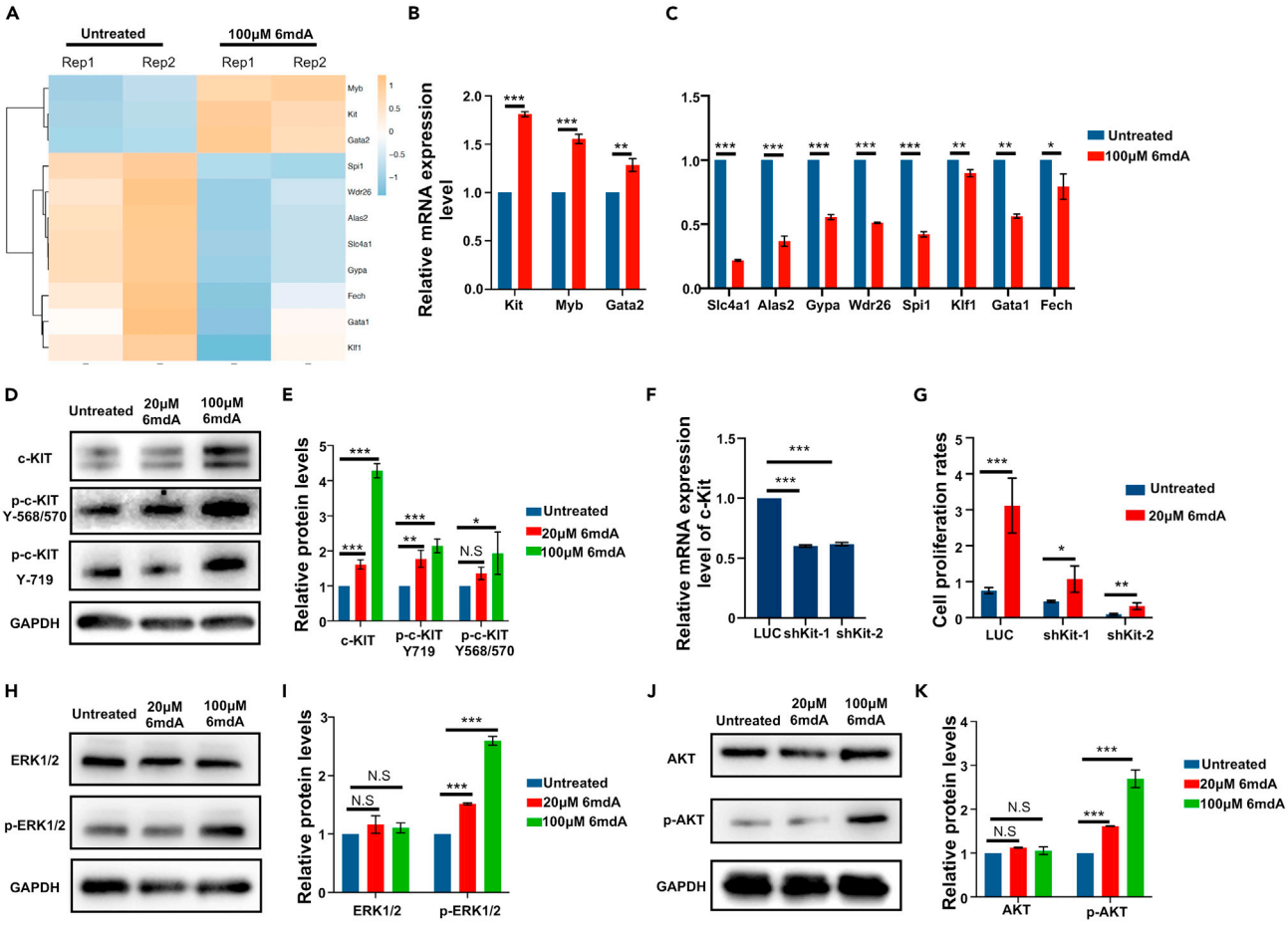

Figure 7. 6mdA upregulates and activates c-Kit in BFU-E cells

(A) Heatmap of the genes involved in the proliferation and differentiation of erythroid progenitors.

(B) mRNA levels of c-Kit, Myb, Gata2 and (C) Slc4a1, Alas2, Gypa, Fech, Wdr26, Gata1, Spi1 and Klf1 as revealed by RT−qPCR. Each treatment contained three replicates.

(D) Western blot analysis of the expression and phosphorylation of c-Kit in BFU-E cells.

(E) Quantitative analysis of expression and phosphorylation of c-Kit protein levels from three independent experiments of BFU-E cells.

(F) c-Kit knockdown validation by RT-qPCR. Each treatment contained three replicates.

(G) Cell proliferation analysis of BFU-E cells after c-Kit knockdown by MTS. Each treatment contained six technical replicates.

(H) Western blot analysis of the expression and phosphorylation of ERK1/2 and (J) AKT on the indicated days in BFU-E cells. (I) Quantitative analysis of the expression and phosphorylation of ERK1/2 and (K) AKT protein levels from three independent experiments of BFU-E cells. Data are presented as mean ± SD. The p values in 7B-7C and 7G were calculated by unpaired t.test. The p values in 7E-7F, 7I and 7K were calculated by one-way ANOVA. (N.S., no significance, *p<0.05, **p<0.01, ***p<0.001).

differentiation by changing the medium to differentiation medium containing high concentrations of EPO. Hemoglobin production and differentiation were analyzed after 3 days of differentiation culture (Figure 8A). Differentiation was analyzed based on the expression of CD71 and Ter119. As shown by flow cytometry analysis, $Ter119^{+}$ cells were not show significant difference after 6mdA treatment in both EPCs and BFU-E cells, indicating that 6mdA treatment in the expansion phase did not have a permanent effect on cell differentiation. After the removal of 6mdA, these cells still differentiated normally, and the differentiation ability was similar to that of the untreated group (Figures 8B and 8C).

In addition, enucleation of differentiated BFU-E cells was also characterized. 6mdA treatment in the expansion phase promoted the enucleation of BFU-E cells after differentiation, from 29% to 39% (Figure 8D). Furthermore, we detected free hemoglobin production in differentiated cultured EPCs and BFU-E cells using tetramethylbenzidine (TMB).[42] As shown in Figure 8E, EPCs induced by 6mdA treatment produced more free hemoglobin after differentiation. Similarly, BFU-E cells induced by 6mdA treatment also

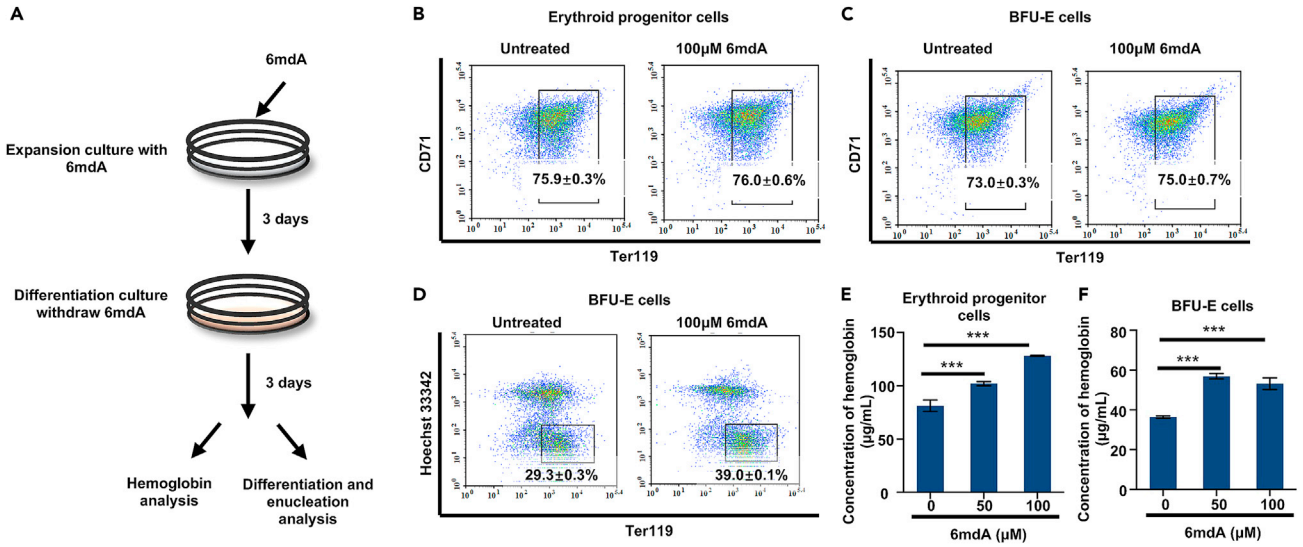

Figure 8. 6mdA does not impair the differentiation of erythroid progenitors

(A) Scheme of the differentiation of EPCs or BFU-E cells.

(B) Ter119^{+} cells according to the surface expression of CD71 and Ter119 of EPCs and (C) BFU-E cells after differentiation. Each treatment had three biological replicates, and the mean ± SD was shown.

(D) Flow cytometry analysis of enucleation of BFU-E cells according to the expression of Ter119 and Hoechst 33342. Each treatment had three biological replicates, and the mean ± SD was shown.

(E) Thefree hemoglobin of EPCs and (F) BFU-E cells after differentiation was analyzed by TMB. Each treatment had three technical replicates. Data are presented as mean ± SD. The p values were calculated by one-way ANOVA (N.S., no significance, *p<0.05, **p<0.01, ***p<0.001).

produced more free hemoglobin after differentiation. (Figures 8E and 8F). Collectively, these findings demonstrate that 6mdA stimulates the hyperproliferation of BFU-E cells, which results in the production of more progenitor cells. These progenitor cells can undergo normal terminal differentiation and produce hemoglobin.

DISCUSSION

Nucleosides and nucleotides are the byproducts formed during RNA/DNA catabolism. These catabolites may function as small bioactive molecules to modulate many cellular events. For example, 2′-deoxyadenosine can inhibit the kinase activity of ATR which in turn induces premature chromatin condensation in hamster BHK21 cells.[43] 2′-Deoxyguanosine can induce growth inhibition and guanosine triphosphate (GTP) accumulation in mature T cell lines and B lymphoblast cell lines.[22,44,45] DNA 6mdA is an important epigenetic modification in prokaryotes[46] and a potential epigenetic mark in multicellular eukaryotes,[47–50] and can be present in the form of 2′-deoxynucleoside or 2′-deoxynucleotide 6mdA during DNA catabolism. The catabolite 6mdA can promote the differentiation of C2C12 cells into osteogenic lineage cells.[51] Moreover, 6mdA induces the differentiation of several mammalian tumor cells, including C6, P19, and PC12 cell lines.[52] 6mdA also enhances the nerve-growth factor-mediated neurite outgrowth of PC12 cells.[53] However, to our knowledge, there have been no reports on the phosphorylation and activation of c-Kit protein caused by 6mdA. Herein, we treated EPCs with different (deoxy)nucleosides and monitored cell proliferation. Surprisingly, we found that 6mdA elevated the proliferation of erythroid progenitors. Further experiments suggested that 6mdA selectively promoted the proliferation of BFU-E cells.

Consistently, 6mdA maintained the expression of genes associated with the proliferation of EPCs. Among these genes, we focused on the receptor tyrosine kinase c-Kit, which plays an important role in EPC proliferation. Of interest, we found that 6mdA treatment significantly upregulated the expression of c-Kit. Furthermore, the phosphorylation of c-Kit was increased, indicating that 6mdA treatment enhanced the activation of c-Kit. However, how 6mdA stimulates the c-Kit activation need further exploration.

As a tyrosine kinase, the activated c-Kit can transduce downstream signaling pathways, including MAPK/ERK and PI3K/AKT. PI3K is activated by c-Kit both directly through binding to Tyr719[39] and indirectly

through binding to the tyrosine phosphorylated adaptor protein Gab2.[54] AKT is a key molecule downstream of PI3 kinase, and the activated AKT promotes the cell survival (anti-apoptotic).[55] The MAPK/ERK signaling pathway stimulated by activated c-Kit starts by recruiting the adaptor protein Grb2 and the guanine nucleotide exchange factor (SOS). SOS activates Ras to recruit and activate Raf by phosphorylation at several sites.[56,57] Activated Raf subsequently phosphorylates downstream MEK1/2 and ERK1/2.[58,59] Activated ERK1/2 promotes cell proliferation by activating multiple transcription factors.[60–62] Importantly, it has been reported that activated MAPK/ERK and PI3K/AKT pathways are involved in the proliferation of hematopoietic progenitors.[63] We found that 6mdA treatment significantly increased the phosphorylation of ERK1/2 and AKT.

According to the World Health Organization (WHO), 118 million donors provide 223 million blood product units per year worldwide.[64] However, the annual demand for blood is 303 million product units. In addition, blood transfusion carries a great risk of disease transmission, including HIV, HBV, HCV, and syphilis transmission. Especially in low-income countries, the risk of HIV transmission is 300 times higher than that in high-income countries. Preparation of red blood cells through bioengineering way has been proposed as a method to solve these problems, and all existing methods of producing red blood cells through bioengineering way involve the proliferation of EPCs. Therefore, all existing methods can benefit from our findings on 6mdA. The effect of 6mdA on enhancing the *ex vivo* proliferation of BFU-E cells implies that 6mdA can serve as a growth factor to improve the production of red blood cells.

Ineffective erythropoiesis can cause anemia such as Diamond-Blackfan anemia (DBA).[65] Despite significant progress in defining the molecular basis of DBA and deepening the understanding of the mechanistic basis of DBA pathophysiology, there has been limited progress in developing new treatment options. Therefore, expect as a supplement for blood transfusion, 6mdA is a potential drug to treat this anemia caused by EPC insufficiency.

In summary, we have demonstrated that 6mdA treatment promotes the proliferation of BFU-E cells by activating the tyrosine kinase c-Kit and its downstream MAPK/ERK and PI3K/AKT pathways. These findings suggest that 6mdA could serve as a growth factor to enhance the proliferation of *ex vivo* cultured EPCs.

Limitations of the study

In this study, we demonstrated that 6mdA treatment promotes the proliferation of EPCs. Our results indicated that 6mdA promotes both mouse fetal liver and bone marrow derived EPCs. The effect of 6mdA on human erythroid cells needs further exploration. We also found that 6mdA treatment maintains the activation of c-Kit and its downstream MAPK and PI3K-AKT signaling pathways. Although the protein directly interacted with 6mdA should be characterized in the future.

STAR★METHODS

Detailed methods are provided in the online version of this paper and include the following:

- KEY RESOURCES TABLE
- RESOURCE AVAILABILITY
  - Lead contact
  - Materials availability
  - Data and code availability
- EXPERIMENTAL MODEL AND SUBJECT DETAILS
  - Animals
  - Cell culture and purification
- METHOD DETAILS
  - MTS assay for cell proliferation
  - EdU incorporation assay for proliferation
  - Colony forming unit assay
  - Flow cytometry
  - Apoptosis assay
  - RNA seq
  - Preparation of lentivirus
  - shRNA mediated knockdown in BFU-E cells

- RNA extraction and RT-qPCR
- Free hemoglobin analysis by reaction with tetramethylbenzidine (TMB)
- Western blot analysis

- QUANTIFICATION AND STATISTICAL ANALYSIS

SUPPLEMENTAL INFORMATION

Supplemental information can be found online at https://doi.org/10.1016/j.isci.2023.106924.

ACKNOWLEDGMENTS

This work is supported by the National Natural Science Foundation of China (22234008, 21927807 and 22021003 to H.L.W.). We are grateful to Professor Wenqiang Yu (Department of General Surgery, Huashan Hospital, Cancer Metastasis Institute, Fudan University) for generosity in providing the plasmids used for the knockdown experiment. We thank Miss Qingjiang Ding for her help in bioinformatic data analysis. We thank Miss Yan Liu for her help in drawing the graphical abstract and Figure 4A.

AUTHOR CONTRIBUTIONS

Project conceived, H.L.W.; methodology, investigation, and validation, Y.L. and Z.Y.L.; writing – Y.L. and H.L.W.; funding acquisition and supervision, H.L.W.

DECLARATION OF INTERESTS

This work has been patented and the acceptance number is 202310511638.0.

Received: February 6, 2023
Revised: April 8, 2023
Accepted: May 15, 2023
Published: May 19, 2023

REFERENCES

1. Tzounakas, V.L., Valsami, S.I., Kriebardis, A.G., Papassideri, I.S., Seghatchian, J., and Antonelou, M.H. (2018). Red cell transfusion in paediatric patients with thalassaemia and sickle cell disease: current status, challenges and perspectives. Transfus. Apher. Sci. *57*, 347–357. https://doi.org/10.1016/j.transci.2018.05.018.

2. Tzounakas, V.L., Seghatchian, J., Grouzi, E., Kokoris, S., and Antonelou, M.H. (2017). Red blood cell transfusion in surgical cancer patients: targets, risks, mechanistic understanding and further therapeutic opportunities. Transfus. Apher. Sci. *56*, 291–304. https://doi.org/10.1016/j.transci.2017.05.015.

3. Lu, S.J., Feng, Q., Park, J.S., Vida, L., Lee, B.S., Strausbauch, M., Wettstein, P.J., Honig, G.R., and Lanza, R. (2008). Biologic properties and enucleation of red blood cells from human embryonic stem cells. Blood *112*, 4475–4484. https://doi.org/10.1182/blood-2008-05-157198.

4. Ma, F., Ebihara, Y., Umeda, K., Sakai, H., Hanada, S., Zhang, H., Zaike, Y., Tsuchida, E., Nakahata, T., Nakauchi, H., and Tsuji, K. (2008). Generation of functional erythrocytes from human embryonic stem cell-derived definitive hematopoiesis. Proc. Natl. Acad. Sci. USA *105*, 13087–13092. https://doi.org/10.1073/pnas.0802220105.

5. Neildez-Nguyen, T.M.A., Wajcman, H., Marden, M.C., Bensidhoum, M., Moncollin, V., Giarratana, M.C., Kobari, L., Thierry, D., and Douay, L. (2002). Human erythroid cells produced ex vivo at large scale differentiate into red blood cells in vivo. Nat. Biotechnol. *20*, 467–472. https://doi.org/10.1038/nbt0502-467.

6. Griffiths, R.E., Kupzig, S., Cogan, N., Mankelow, T.J., Betin, V.M.S., Trakarnsanga, K., Massey, E.J., Lane, J.D., Parsons, S.F., and Anstee, D.J. (2012). Maturing reticulocytes internalize plasma membrane in glycophorin A-containing vesicles that fuse with autophagosomes before exocytosis. Blood *119*, 6296–6306. https://doi.org/10.1182/blood-2011-09-376475.

7. Giarratana, M.C., Rouard, H., Dumont, A., Kiger, L., Safeukui, I., Le Pennec, P.Y., François, S., Trugnan, G., Peyrard, T., Marie, T., et al. (2011). Proof of principle for transfusion of in vitro-generated red blood cells. Blood *118*, 5071–5079. https://doi.org/10.1182/blood-2011-06-362038.

8. Lapillonne, H., Kobari, L., Mazurier, C., Tropel, P., Giarratana, M.C., Zanella-Cleon, I., Kiger, L., Wattenhofer-Donzé, M., Puccio, H., Hebert, N., et al. (2010). Red blood cell generation from human induced pluripotent stem cells: perspectives for transfusion medicine. Haematologica *95*, 1651–1659. https://doi.org/10.3324/haematol.2010.023556.

9. Qu, X., Zhang, S., Wang, S., Wang, Y., Li, W., Huang, Y., Zhao, H., Wu, X., An, C., Guo, X., et al. (2018). TET2 deficiency leads to stem cell factor–dependent clonal expansion of dysfunctional erythroid progenitors. Blood *132*, 2406–2417. https://doi.org/10.1182/blood-2018-05-853291.

10. Dzierzak, E., and Philipsen, S. (2013). Erythropoiesis: development and differentiation. Cold Spring Harb. Perspect. Med. *3*, a011601–a011616. https://doi.org/10.1101/cshperspect.a011601.

11. Nocka, K., Majumder, S., Chabot, B., Ray, P., Cervone, M., Bernstein, A., and Besmer, P. (1989). Expression of c-kit gene products in known cellular targets of W mutations in normal and W mutant mice–evidence for an impaired c-kit kinase in mutant mice. Genes Dev. *3*, 816–826. https://doi.org/10.1101/gad.3.6.816.

12. Krantz, S.B. (1991). Erythropoietin. Blood *77*, 419–434. https://doi.org/10.1182/blood.V77.3.419.419.

13. Yuzawa, S., Opatowsky, Y., Zhang, Z., Mandiyan, V., Lax, I., and Schlessinger, J. (2007). Structural basis for activation of the receptor tyrosine kinase KIT by stem cell factor. Cell *130*, 323–334. https://doi.org/10.1016/j.cell.2007.05.055.

14. Kapur, R., Chandra, S., Cooper, R., McCarthy, J., and Williams, D.A. (2002). Role of p38 and ERK MAP kinase in proliferation of erythroid progenitors in response to stimulation by soluble and membrane isoforms of stem cell

factor. Blood *100*, 1287–1293. https://doi.org/10.1182/blood.V100.4.1287.h81602001287_1287_1293.

15. Deshpande, S., Bosbach, B., Yozgat, Y., Park, C.Y., Moore, M.A.S., and Besmer, P. (2013). KIT receptor gain-of-function in hematopoiesis enhances stem cell self-renewal and promotes progenitor cell expansion. Stem Cell. *31*, 1683–1695. https://doi.org/10.1002/stem.1419.

16. Munugalavadla, V., and Kapur, R. (2005). Role of c-Kit and erythropoietin receptor in erythropoiesis. Crit. Rev. Oncol. Hematol. *54*, 63–75. https://doi.org/10.1016/j.critrevonc.2004.11.005.

17. Couch, T., Murphy, Z., Getman, M., Kurita, R., Nakamura, Y., and Steiner, L.A. (2019). Human erythroblasts with c-Kit activating mutations have reduced cell culture costs and remain capable of terminal maturation. Exp. Hematol. *74*, 19–24.e4. https://doi.org/10.1016/j.exphem.2019.04.001.

18. Zochodne, B., Truong, A.H., Stetler, K., Higgins, R.R., Howard, J., Dumont, D., Berger, S.A., and Ben-David, Y. (2000). Epo regulates erythroid proliferation and differentiation through distinct signaling pathways: implication for erythropoiesis and Friend virus-induced erythroleukemia. Oncogene *19*, 2296–2304. https://doi.org/10.1038/sj.onc.1203590.

19. Flygare, J., Rayon Estrada, V., Shin, C., Gupta, S., and Lodish, H.F. (2011). HIF1alpha synergizes with glucocorticoids to promote BFU-E progenitor self-renewal. Blood *117*, 3435–3444. https://doi.org/10.1182/blood-2010-07-295550.

20. Uoshima, N., Ozawa, M., Kimura, S., Tanaka, K., Wada, K., Kobayashi, Y., and Kondo, M. (1995). Changes in c-Kit expression and effects of SCF during differentiation of human erythroid progenitor cells. Br. J. Haematol. *91*, 30–36. https://doi.org/10.1111/j.1365-2141.1995.tb05240.x.

21. Cekic, C., Sag, D., Day, Y.J., and Linden, J. (2013). Extracellular adenosine regulates naive T cell development and peripheral maintenance. J. Exp. Med. *210*, 2693–2706. https://doi.org/10.1084/jem.20130249.

22. Weiler, M., Schmetzer, H., Braeu, M., and Buhmann, R. (2016). Inhibitory effect of extracellular purine nucleotide and nucleoside concentrations on T cell proliferation. Exp. Cell Res. *349*, 1–14. https://doi.org/10.1016/j.yexcr.2016.05.017.

23. Puchalowicz, K., Tarnowski, M., Tkacz, M., Chlubek, D., Klos, P., and Dziedziejko, V. (2020). Extracellular adenine nucleotides and adenosine modulate the growth and survival of THP-1 leukemia cells. Int. J. Mol. Sci. *21*, 1–16. https://doi.org/10.3390/ijms21124425.

24. Schooley, J.C., and Mahlmann, L.J. (1975). Adenosine, AMP, cyclic AMP, theophylline and the action and production of erythropoietin. Proc. Soc. Exp. Biol. Med. *150*, 215–219.

25. McIver, S.C., Hewitt, K.J., Gao, X., Mehta, C., Zhang, J., and Bresnick, E.H. (2018). Dissecting regulatory mechanisms using mouse fetal liver-derived erythroid cells. Methods Mol. Biol. *1698*, 67–89. https://doi.org/10.1007/978-1-4939-7428-3_4.

26. Vizirianakis, I.S., and Tsiftsoglou, A.S. (1995). N6-methyladenosine inhibits murine erythroleukemia cell maturation by blocking methylation of RNA and memory via conversion to S-(N6-methyl)-adenosylhomocysteine. Biochem. Pharmacol. *50*, 1807–1814. https://doi.org/10.1016/0006-2952(95)02056-x.

27. Tsai, F.Y., and Orkin, S.H. (1997). Transcription factor GATA-2 is required for proliferation/survival of early hematopoietic cells and mast cell formation, but not for erythroid and myeloid terminal differentiation. Blood *89*, 3636–3643. https://doi.org/10.1182/blood.V89.10.3636.

28. Mucenski, M.L., McLain, K., Kier, A.B., Swerdlow, S.H., Schreiner, C.M., Miller, T.A., Pietryga, D.W., Scott, W.J., and Potter, S.S. (1991). A functional c-myb gene is required for normal murine fetal hepatic hematopoiesis. Cell *65*, 677–689. https://doi.org/10.1016/0092-8674(91)90099-K.

29. Zhen, R., Moo, C., Zhao, Z., Chen, M., Feng, H., Zheng, X., Zhang, L., Shi, J., and Chen, C. (2020). Wdr26 regulates nuclear condensation in developing erythroblasts. Blood *135*, 208–219. https://doi.org/10.1182/blood.2019002165.

30. Ferreira, G.C., and Gong, J. (1995). 5-Aminolevulinate synthase and the first step of heme biosynthesis. J. Bioenerg. Biomembr. *27*, 151–159. https://doi.org/10.1007/BF02110030.

31. Ferreira, G.C., Franco, R., Lloyd, S.G., Moura, I., Moura, J.J., and Huynh, B.H. (1995). Structure and function of ferrochelatase. J. Bioenerg. Biomembr. *27*, 221–229. https://doi.org/10.1007/BF02110037.

32. Kalli, A.C., and Reithmeier, R.A.F. (2022). Organization and dynamics of the red blood cell band 3 anion exchanger SLC4A1: insights from molecular dynamics simulations. Front. Physiol. *13*, 817945–818013. https://doi.org/10.3389/fphys.2022.817945.

33. Back, J., Dierich, A., Bronn, C., Kastner, P., and Chan, S. (2004). PU.1 determines the self-renewal capacity of erythroid progenitor cells. Blood *103*, 3615–3623. https://doi.org/10.1182/blood-2003-11-4089.

34. Gregory, T., Yu, C., Ma, A., Orkin, S.H., Blobel, G.A., and Weiss, M.J. (1999). GATA-1 and erythropoietin cooperate to promote erythroid cell survival by regulating bcl-xL expression. Blood *94*, 87–96. https://doi.org/10.1182/blood.V94.1.87.413k41_87_96.

35. Gnanapragasam, M.N., and Bieker, J.J. (2017). Orchestration of late events in erythropoiesis by KLF1/EKLF. Curr. Opin. Hematol. *24*, 183–190. https://doi.org/10.1097/MOH.0000000000000327.

36. Lennartsson, J., Blume-Jensen, P., Hermanson, M., Pontén, E., Carlberg, M., and Rönnstrand, L. (1999). Phosphorylation of Shc by Src family kinases is necessary for stem cell factor receptor/c-kit mediated activation of the Ras/MAP kinase pathway and c-fos induction. Oncogene *18*, 5546–5553. https://doi.org/10.1038/sj.onc.1202929.

37. Ueda, S., Mizuki, M., Ikeda, H., Tsujimura, T., Matsumura, I., Nakano, K., Daino, H., Honda Zi, Z.i., Sonoyama, J., Shibayama, H., et al. (2002). Critical roles of c-Kit tyrosine residues 567 and 719 in stem cell factor–induced chemotaxis: contribution of src family kinase and PI3-kinase on calcium mobilization and cell migration. Blood *99*, 3342–3349. https://doi.org/10.1182/blood.V99.9.3342.

38. Timokhina, I., Kissel, H., Stella, G., and Besmer, P. (1998). Kit signaling through PI 3-kinase and Src kinase pathways: an essential role for Rac1 and JNK activation in mast cell proliferation. EMBO J. *17*, 6250–6262. https://doi.org/10.1093/emboj/17.21.6250.

39. Hong, L., Munugalavadla, V., and Kapur, R. (2004). c-Kit-mediated overlapping and unique functional and biochemical outcomes via diverse signaling pathways. Mol. Cell Biol. *24*, 1401–1410. https://doi.org/10.1128/MCB.24.3.1401-1410.2004.

40. Zsebo, K.M., Williams, D.A., Geissler, E.N., Broudy, V.C., Martin, F.H., Atkins, H.L., Hsu, R.-Y., Birkett, N.C., Okino, K.H., Murdock, D.C., et al. (1990). Stem cell factor is encoded at the Sl locus of the mouse and is the ligand for the c-kit tyrosine kinase receptor. Cell *63*, 213–224. https://doi.org/10.1016/0092-8674(90)90302-U.

41. Comazzetto, S., Murphy, M.M., Berto, S., Jeffery, E., Zhao, Z., and Morrison, S.J. (2019). Restricted hematopoietic progenitors and erythropoiesis require SCF from leptin Receptor+ niche cells in the bone marrow. Cell Stem Cell *24*, 477–486.e6. https://doi.org/10.1016/j.stem.2018.11.022.

42. Raftos, J.E., Stewart, I.M., and Lovric, V.A. (1986). Supernatant hemoglobin determinations after prolonged blood storage. Pathology *18*, 123–126. https://doi.org/10.3109/00313028609090838.

43. Nishijima, H., Nishitani, H., Saito, N., and Nishimoto, T. (2003). Caffeine mimics adenine and 2′-deoxyadenosine, both of which inhibit the guanine-nucleotide exchange activity of RCC1 and the kinase activity of ATR. Gene Cell. *8*, 423–435. https://doi.org/10.1046/j.1365-2443.2003.00644.x.

44. Mann, G.J., and Fox, R.M. (1986). Deoxyadenosine triphosphate as a mediator of deoxyguanosine toxicity in cultured T lymphoblasts. J. Clin. Invest. *78*, 1261–1269. https://doi.org/10.1172/JCI112710.

45. Sidi, Y., and Mitchell, B.S. (1984). 2′-deoxyguanosine toxicity for B and mature T lymphoid cell lines is mediated by guanine ribonucleotide accumulation. J. Clin. Invest. *74*, 1640–1648. https://doi.org/10.1172/JCI111580.

46. Dunn, D.B., and Smith, J.D. (1958). The occurrence of 6-methylaminopurine in deoxyribonucleic acids. Biochem. J. *68*, 627–636. https://doi.org/10.1042/bj0680627.

47. Zhang, G., Huang, H., Liu, D., Cheng, Y., Liu, X., Zhang, W., Yin, R., Zhang, D., Zhang, P., Liu, J., et al. (2015). N6-methyladenine DNA modification in Drosophila. Cell *161*, 893–906. https://doi.org/10.1016/j.cell.2015.04.018.

48. Xiao, C.L., Zhu, S., He, M., Chen, D., Zhang, Q., Chen, Y., Yu, G., Liu, J., Xie, S.Q., Luo, F., et al. (2018). N(6)-Methyladenine DNA modification in the human genome. Mol. Cell *71*, 306–318.e7. https://doi.org/10.1016/j.molcel.2018.06.015.

49. Fu, Y., Luo, G.Z., Chen, K., Deng, X., Yu, M., Han, D., Hao, Z., Liu, J., Lu, X., Dore, L.C., et al. (2015). N6-methyldeoxyadenosine marks active transcription start sites in Chlamydomonas. Cell *161*, 879–892. https://doi.org/10.1016/j.cell.2015.04.010.

50. Greer, E.L., Blanco, M.A., Gu, L., Sendinc, E., Liu, J., Aristizábal-Corrales, D., Hsu, C.H., Aravind, L., He, C., and Shi, Y. (2015). DNA methylation on N6-adenine in C. elegans. Cell *161*, 868–878. https://doi.org/10.1016/j.cell.2015.04.005.

51. Charles, M.P., Ravanat, J.L., Adamski, D., D'Orazi, G., Cadet, J., Favier, A., Berger, F., and Wion, D. (2004). N(6)-Methyldeoxyadenosine, a nucleoside commonly found in prokaryotes, induces C2C12 myogenic differentiation. Biochem. Biophys. Res. Commun. *314*, 476–482. https://doi.org/10.1016/j.bbrc.2003.12.132.

52. Ratel, D., Boisseau, S., Davidson, S.M., Ballester, B., Mathieu, J., Morange, M., Adamski, D., Berger, F., Benabid, A.L., and Wion, D. (2001). The bacterial nucleoside N(6)-methyldeoxyadenosine induces the differentiation of mammalian tumor cells. Biochem. Biophys. Res. Commun. *285*, 800–805. https://doi.org/10.1006/bbrc.2001.5240.

53. Charles, M.P., Adamski, D., Kholler, B., Pelletier, L., Berger, F., and Wion, D. (2003). Induction of neurite outgrowth in PC12 cells by the bacterial nucleoside N6-methyldeoxyadenosine is mediated through adenosine A2a receptors and via cAMP and MAPK signaling pathways. Biochem. Biophys. Res. Commun. *304*, 795–800. https://doi.org/10.1016/s0006-291x(03)00666-1.

54. Nishida, K., Wang, L., Morii, E., Park, S.J., Narimatsu, M., Itoh, S., Yamasaki, S., Fujishima, M., Ishihara, K., Hibi, M., et al. (2002). Requirement of Gab2 for mast cell development and KitL/c-Kit signaling. Blood *99*, 1866–1869. https://doi.org/10.1182/blood.V99.5.1866.

55. Yasuda, A., Sawai, H., Takahashi, H., Ochi, N., Matsuo, Y., Funahashi, H., Sato, M., Okada, Y., Takeyama, H., and Manabe, T. (2007). Stem cell factor/c-kit receptor signaling enhances the proliferation and invasion of colorectal cancer cells through the PI3K/Akt pathway. Dig. Dis. Sci. *52*, 2292–2300. https://doi.org/10.1007/s10620-007-9759-7.

56. Moodie, S.A., Willumsen, B.M., Weber, M.J., and Wolfman, A. (1993). Complexes of Ras.GTP with Raf-1 and mitogen-activated protein kinase kinase. Science *260*, 1658–1661. https://doi.org/10.1126/science.8503013.

57. Vojtek, A.B., Hollenberg, S.M., and Cooper, J.A. (1993). Mammalian Ras interacts directly with the serine/threonine kinase raf. Cell *74*, 205–214. https://doi.org/10.1016/0092-8674(93)90307-C.

58. Whitmarsh, A.J., and Davis, R.J. (1998). Structural organization of MAP-kinase signaling modules by scaffold proteins in yeast and mammals. Trends Biochem. Sci. *23*, 481–485. https://doi.org/10.1016/S0968-0004(98)01309-7.

59. Schaeffer, H.J., and Weber, M.J. (1999). Mitogen-activated protein kinases: specific messages from ubiquitous messengers. Mol. Cell Biol. *19*, 2435–2444. https://doi.org/10.1128/MCB.19.4.2435.

60. Gille, H., Sharrocks, A.D., and Shaw, P.E. (1992). Phosphorylation of transcription factor p62TCF by MAP kinase stimulates ternary complex formation at c-fos promoter. Nature *358*, 414–417. https://doi.org/10.1038/358414a0.

61. Chen, R.H., Sarnecki, C., and Blenis, J. (1992). Nuclear localization and regulation of erk- and rsk-encoded protein kinases. Mol. Cell Biol. *12*, 915–927. https://doi.org/10.1128/mcb.12.3.915-927.1992.

62. Zhao, J., Yuan, X., Frödin, M., and Grummt, I. (2003). ERK-dependent phosphorylation of the transcription initiation factor TIF-IA is required for RNA Polymerase I transcription and cell growth. Mol. Cell *11*, 405–413. https://doi.org/10.1016/S1097-2765(03)00036-4.

63. Wandzioch, E., Edling, C.E., Palmer, R.H., Carlsson, L., and Hallberg, B. (2004). Activation of the MAP kinase pathway by c-Kit is PI-3 kinase dependent in hematopoietic progenitor/stem cell lines. Blood *104*, 51–57. https://doi.org/10.1182/blood-2003-07-2554.

64. Organization, W.H. (2022). Global Status Report on Blood Safety and Availability 2021.

65. Da Costa, L., Leblanc, T., and Mohandas, N. (2020). Diamond-Blackfan anemia. Blood *136*, 1262–1273. https://doi.org/10.1182/blood.2019000947.

STAR★METHODS

KEY RESOURCES TABLE

REAGENT or RESOURCE	SOURCE	IDENTIFIER
Antibodies		
Biotin anti-mouse lineage panel	BioLegend	Cat# 133307; RRID:AB_11124348
Biotin anti-mouse CD19	BioLegend	Cat# 115504; RRID:AB_2936614
Biotin anti-mouse CD71	BioLegend	Cat# 113803; RRID:AB_313564
Biotin anti-mouse CD34	BioLegend	Cat# 128604; RRID:AB_1236371
Biotin anti-mouse CD41	BioLegend	Cat# 133930; RRID:AB_2572133
Biotin anti-mouse Sca-1	BioLegend	Cat# 108104; RRID:AB_313341
Biotin anti-mouse CD16/32	BioLegend	Cat# 101303; RRID:AB_312802
PE anti-mouse TER-119	BioLegend	Cat# 116208; RRID:AB_313709
APC anti-mouse CD117 (c-Kit)	BioLegend	Cat# 135108; RRID:AB_2028407
PE/Cy7 anti-mouse CD71	BioLegend	Cat# 113812; RRID:AB_2203382
c-Kit rabbit mAb	Cell Signaling Technology	Cat# 3074; RRID:AB_1147633
Phospho-c-Kit (Tyr719) antibody	Cell Signaling Technology	Cat# 3391; RRID:AB_2131153
Phospho-c-Kit (Tyr568/570) antibody	Cell Signaling Technology	Cat# 48347; RRID:AB_2799336
p44/42 MAPK (Erk1/2) rabbit mAb	Cell Signaling Technology	Cat# 4695; RRID:AB_390779
Phospho-p44/42 MAPK (Erk1/2) (Thr202/ Tyr204) rabbit mAb	Cell Signaling Technology	Cat# 4370; RRID:AB_2315112
Akt (pan) rabbit mAb	Cell Signaling Technology	Cat# 4691; RRID:AB_915783
Phospho-Akt (Ser473) rabbit mAb	Cell Signaling Technology	Cat# 4060; RRID:AB_2315049
Stat5 rabbit mAb	Cell Signaling Technology	Cat# 94205; RRID:AB_2737403
Phospho-Stat5 (Tyr694) rabbit mAb	Cell Signaling Technology	Cat# 4322; RRID:AB_10544692
Anti-rabbit IgG	Cell Signaling Technology	Cat# 7074; RRID:AB_2099233
Anti-GAPDH	Gene-Protein Link	Cat# P01L081
Chemicals, peptides, and recombinant proteins		
N6-methyldeoxyadenosine (6mdA)	Sigma-Aldrich	Cat# M2389
2′-Deoxyadenosine (dA)	Sigma-Aldrich	Cat# D8668
2′-Deoxyguanosine (dG)	J&K Scientific	Cat# 240184
2′-Deoxycytidine (dC)	J&K Scientific	Cat# 206550
2′-Deoxythmidine (dT)	Solarbio Life Science	Cat# T8081
Adenosine (rA)	Sigma-Aldrich	Cat# A9251
Cytidine	Sigma-Aldrich	Cat# C122106
Uridine	Sigma-Aldrich	Cat# U3750
Guanosine	Sigma-Aldrich	Cat# G6752
N6-methyladenosine	Aladdin	Cat# N191760
Imatinib (STI571) Mesylate	Selleck	Cat# S1026
Selumetinib	Selleck	Cat# S1008
U0126-EtOH	Selleck	Cat# S1102
LY294002	Selleck	Cat# S1105
Streptavidin Microbeads	Miltenyi Biotec	Cat# 130-048-101
StemPro-34 SFM	Thermo Fisher	Cat# 10639011
Human EPO	PeproTech	Cat# 100-64-10
Murine SCF	PeproTech	Cat# 250-03-10

(*Continued on next page*)

Continued

REAGENT or RESOURCE	SOURCE	IDENTIFIER
Dexamethasone	Sigma-Aldrich	Cat# D4902
IMDM (glutamine-free)	Hyclone	Cat# SH30259
PFHM II	Thermo Fisher	Cat# 12040077
TRIzol	Thermo Fisher	Cat# 15596026
Critical commercial assays		
CellTiter 96® AQueous One Solution Reagent	Promega	Cat# G3580
Click-iT® EdU Imaging Kit with Alexa Fluor® 594 Azides	Thermo Fisher	Cat# C10338
Deposited data		
RNA seq	This study	https://ngdc.cncb.ac.cn/search/?dbId=&q=CRA010146
Oligonucleotides		
See Table S1		
Recombinant DNA		
pLKO.1-Puro	Wenqiang Yu's laboratory	N/A
pMDL	Wenqiang Yu's laboratory	N/A
VSVG	Wenqiang Yu's laboratory	N/A
REV	Wenqiang Yu's laboratory	N/A
Software and algorithms		
NovoExpress	ACEA	N/A
Alliance Q9 ATMO LIGHT	UVITEC	N/A
Prism9	GraphPad	https://www.graphpad.com/scientific-software/prism/

RESOURCE AVAILABILITY

Lead contact

Further information and requests for resources and reagents should be directed to and will be fulfilled by the lead contact, Hailin Wang (hlwang@rcees.ac.cn).

Materials availability

This study did not generate new unique reagents.

Data and code availability

- All data reported in this paper will be shared by the lead contact upon request.
- This paper does not report original code.
- Any additional information required to reanalyze the data reported in this paper is available from the lead contact upon request.

EXPERIMENTAL MODEL AND SUBJECT DETAILS

Animals

All animal procedures were approved by and performed according to the guidelines of the Animal Ethics and Welfare Committee of Research Center for Eco-Environment Sciences, Chinese Academy of Science, approval No. AEWC-RCEES-2021049.

Cell culture and purification

Erythroid precursor cells were purified as McIver et al. described.[25] Isolated erythroid precursor cells from E13.5 fetal liver by negative selection using magnetic beads, according to the manufacturer's instructions. Specifically, after isolating fetal liver cells from E13.5 embryos of pregnant C57/6J mice, 2 μL of each antibody in the biotin anti-mouse lineage panel and 2 μL of Streptavidin Microbeads (Miltenyi Biotec) per million cells were used. Lin^- cells were collected by passing the labeled fetal liver cells through an LS column. Then, the cells were incubated with biotin anti-mouse CD19 and biotin anti-mouse CD71 to obtain $Lin^-CD19^-CD71^-$ erythroid precursor cells.

For BFU-E or CFU-E cell purification, E13.5 fetal liver cells were isolated from pregnant C57/6J mice and incubated with a biotin anti-mouse lineage panel, followed by biotin anti-mouse CD34, biotin anti-mouse CD41, biotin anti-mouse Sca-1, and biotin anti-mouse CD16/32 to deplete $Lin^+CD34^+CD41^+Sca^+CD16/32^+$ cells. The remaining cells were incubated with APC anti-mouse c-Kit and PE-CY7 anti-mouse CD71 for flow cytometry to obtain more accurate BFU-E and CFU-E cells.

Purified EPCs or BFU-E cells were cultured in expansion medium or differentiation medium as described by McIver et al. The expansion medium was StemPro-34 (Thermo Fisher) with 1x nutrient supplement, 2 mM L-glutamine, 1% penicillin/streptomycin, 100 μM monothioglycerol, 1 μM dexamethasone, 0.5 U/mL of erythropoietin (EPO), and 100 ng/mL recombinant SCF. The differentiation medium was IMDM (glutamine-free) supplemented with 20% FBS, 5% PFHM II, 2 mM L-glutamine, 1% penicillin/streptomycin, 100 μM monothioglycerol, and 6 U/mL EPO. The cells were cultured in a humidified incubator at 37 °C with 5% CO_2.

METHOD DETAILS

MTS assay for cell proliferation

A total of 1.5 x 10^4 cells were seeded in a 12-well cell culture cluster (Corning) and incubated in 1.5 mL expansion medium. The cells were treated with deoxyribonucleoside or nucleoside derivatives at different concentrations. The relative cell proliferation was assessed in an assay using MTS (3-(4,5-dimethylthiazol-2-yl)-5-(3-carboxymethoxyphenyl)-2-(4-sulfophenyl)-2H-tetrazolium). Briefly, the MTS working solution was prepared according to the manufacturer's instructions, 600 μL of IMDM medium supplemented with 120 μL of CellTiter 96 AQueous One Solution Reagent (Promega). The cells were collected and resuspended in MTS working solution and divided equally among the six wells of a 96-well cell culture cluster. The plate was incubated at 37 °C for 2 h in humidified, 5% CO_2. The absorbance at 490 nm was recorded using a Synergy H1 multifunctional microporous plate detector (BioTek) with a 96-well plate reader.

"Relative cell proliferation" was calculated as follows:

$$\text{Relative cell proliferation} = \left[A_{(\text{sample in indicated days})} - A_{(\text{blank})}\right] / \left[A_{(\text{sample in day 0})} - A_{(\text{blank})}\right]$$

$A_{(\text{sample in indicated days})}$ represents the optical density (OD490) value of cells treated with vehicle, 6mdA, or other nucleosides in the indicated expansion days, and $A_{(\text{blank})}$ represents the OD490 value of the blank group containing only culture medium and MTS solution (without cells). $A_{(\text{sample in day 0})}$ represents the OD490 value of the initiation cells seeded on day 0. The initial number of seeded cells of different treatments was the same as that on day 0.

EdU incorporation assay for proliferation

Before being seeded in eight-chamber slides, 5x10^5 cells were treated with 6mdA nucleosides for the indicated times. The cells were incubated with EdU for 20 min and fixed with 4% paraformaldehyde. The cells were permeabilized with 0.1% Triton X-100 in PBS for 15 min and washed twice with PBS. Then the cells were incubated with fluorescent azide solution for 30 min (Click-iT EdU Imaging Kit with Alexa Fluor 555 Azides) for incorporated EdU detection. After washing with PBS, slides were covered with 4′,6-diamidino-2-phenylindole (DAPI) (Beyotime). Fluorescence images were captured using SP5 confocal spectral microscopy (Leica). The EdU signal was visualized with excitation at 550 nm and emission at 565 nm, and the DAPI signal was visualized with excitation at 350 nm and emission at 461 nm. For flow cytometry analysis of EdU incorporation, 5x10^5 cells were fixed with 4% paraformaldehyde and permeabilized with 0.1% Triton X-100 after incubation with 1 μM EdU for 20 min. After staining with Yefluor 488 Azide (Yeasen), the cells were resuspended in PBS for flow cytometry analysis with a BD Aria II flow cytometer (BD Biosciences).

Colony forming unit assay

BMCs were isolated from 10-week-old adult C57/6J mice. BMCs ($3x10^4$) were mixed with 1.2 mL of MethoCult media (STEMCELL) in 35 mm cell culture dishes. After 14 days later, clone numbers and clonal morphology were recorded.

Flow cytometry

Ex vivo-cultured erythroid precursor cells were collected at 3 and 6 days after 6mdA treatment for analyses of differentiation and enucleation, respectively. To analyze maturation, cells were collected and washed twice with PBS. The cells were resuspended and stained with APC anti-mouse c-Kit (CD117), PE anti-mouse TER-119, PE/Cy7 anti-mouse CD71 and APC/CY7 anti-mouse CD44, incubated on ice for 15 min, and then washed off. The cells were resuspended in PBS for flow cytometry analysis with a BD Aria II flow cytometer (BD Biosciences). Enucleation of differentiated cells was analyzed based on the expression of Ter-119 and Hoechst 33342.

Apoptosis assay

The apoptosis of EPCs after 6 days of expansion was analyzed using an Annexin-V and propidium iodide staining kit (Solarbio). Briefly, cells were collected and incubated with Annexin-V. After propidium iodide was added, the cells were immediately analyzed by flow cytometry. The Annexin-V signal was visualized with excitation at 488 nm and emission at 519 nm, and the propidium iodide signal was visualized with excitation at 490 nm and emission at 615 nm.

RNA seq

For RNA seq, *ex vivo*-cultured 2×10^6 EPCs and BFU-E cells were collected after 4 days and 6 days of 6mdA treatment, respectively. RNA-sequencing (RNA-seq) libraries were constructed and subjected to Illumina sequencing. The raw reads were aligned to the mouse reference genome (mm10). Gene expression was analyzed by Feature Counts. The complete datasets are available at the National Genomics Data Center (NGDC) under accession number of CRA010146 (https://ngdc.cncb.ac.cn/search/?dbId=&q=CRA010146)

Preparation of lentivirus

Small hairpin RNA (shRNA) against luciferase or the target gene was annealed and connected to the pLKO.1 vector. Lentivirus particles were produced by cotransfecting 293T cells with pMDL, VSVG, REV, and the pLKO.1 vector with shRNA. The supernatant containing viral particles was collected twice after 24 h and 48 h of transfection. The collected supernatant was filtered through 0.2 μm cellulose acetate filters, and a quarter volume of PEG8000-NaCl solution was added. The virus particles were concentrated by centrifugation at 4000rpmat room temperature. The pellet from 20 mL of supernatant was resuspended in 200 μL of expansion medium. The shRNA sequences used for knockdown of c-Kit are listed in the Table S1.

shRNA mediated knockdown in BFU-E cells

100 μL of virus supernatant was added to $1x10^5$ BFU-E cells. The mixture was centrifuged at 1500 x g for 1 h at room temperature to allow close contact between the virus and the cells. After 48 h of incubation, 1 μg/mL puromycin was added to the cell culture medium for selection. At 48 h following the addition of puromycin, untransduced cells were routinely killed, and the relative cell proliferation and knockdown efficiency were determined by MTS and RT-qPCR assays, respectively.

RNA extraction and RT-qPCR

Total RNA of *ex vivo* cultured EPCs with or without 6mdA treatment was extracted with TRIzol reagent. 500 ng of total RNA was used for cDNA synthesis by using the HiScript III first Strand cDNA Synthesis Kit (Vazyme). Real-time PCR was performed using AceQ qPCR SYBR Green Master Mix (Vazyme) following the manufacturer's instructions on a Roche LightCycler 480II real-time PCR System (Roche). The expression of genes was normalized to that of Gapdh. The primer sequences are listed in Table S1.

Free hemoglobin analysis by reaction with tetramethylbenzidine (TMB)

Free hemoglobin production after differentiation was analyzed by reaction with TMB. Briefly, 2 million EPCs or 1 million BFU-E cells were collected and treated with 1X RBC lysis buffer (Life Technologies Corporation)

and incubated at room temperature for 5 min. After centrifugation for 5minat 300 x g, the supernatant was collected and added to a 96-well cell culture cluster. Then, 100 μL of TMB solution (Solarbio) was added and incubated at room temperature for 15 min. After adding 50 μL of termination buffer (Solarbio), the absorbance was recorded at 450 nm and 630 nm using a Synergy H1 multifunctional microporous plate detector (BioTek) with a 96-well plate reader. Quantification was performed according to the hemoglobin standard.

Western blot analysis

The expression of c-Kit, ERK1/2, AKT, STAT5, and phospho-*c*-Kit, phospho-ERK1/2, phospho-AKT, and phospho-STAT5 was analyzed by western blot. Briefly, the EPCs were harvested after 2, 4, and 6 days with or without 6mdA treatment. The cells were lysed with RIPA lysis buffer supplemented with 1% PMSF, 1% phosphatase inhibitors, and 1% protease inhibitor cocktail. Protein quantification was performed using a BCA protein assay kit. Equal amounts of proteins were separated by NuPAGE 4–12% bis-tris gel in MOPS SDS running buffer. Subsequently, the proteins were transferred onto a 0.45 μm PVDF membrane. After blocking with 5% skim milk powder-TBST for 1 h, the membrane was incubated with c-Kit rabbit antibody, phospho-*c*-Kit (Tyr719) antibody, phospho-*c*-Kit (Tyr568/570) antibod, ERK rabbit antibody, *p*-ERK rabbit antibody, AKT rabbit antibody, phospho-AKT rabbit antibody, STAT5 rabbit antibody, phospho-STAT5 rabbit antibody at a 1:1000 dilution and with a GAPDH rabbit antibody at a 1:2000 dilution in 5% BSA-TBST overnight at 4°C. Each membrane was washed three times with TBST and incubated with anti-rabbit IgG, HRP-linked secondary antibody at a 1:2000 dilution for 4hat room temperature. After washing three times with TBST, the membrane was imaged by an Alliance Q9 ATMO LIGHT (UVITEC).

QUANTIFICATION AND STATISTICAL ANALYSIS

Data are expressed as average +/− standard deviation (SD). Statistical significance was evaluated by unpaired Student's *t* test or one-way ANOVA, ns: not significant, *$p<0.05$, **$p<0.01$, and ***$p<0.001$.